Deep-Sea Research Part I 143 (2019) 85–103

Contents lists available at ScienceDirect

Deep-Sea Research Part I

journal homepage: www.elsevier.com/locate/dsri

Connectivity modelling of areas closed to protect vulnerable marine ecosystems in the northwest Atlantic

Ellen Kenchington[a,*], Zeliang Wang[a], Camille Lirette[a], Francisco Javier Murillo[a], Javier Guijarro[a], Igor Yashayaev[a], Manuel Maldonado[b]

[a] Ocean and Ecosystem Sciences Division, Department of Fisheries and Oceans, Bedford Institute of Oceanography, 1 Challenger Dr., Dartmouth, N.S., Canada
[b] Department of Marine Ecology, Center for Advanced Studies of Blanes (CEAB-CSIC), Accés a la Cala St. Francesc, 14, Girona, Spain

ARTICLE INFO

Keywords:
Vulnerable marine ecosystems
Connectivity
Flemish Cap
Grand Banks
Particle tracking models
Protected area networks

ABSTRACT

Over the course of the past decade, in response to United Nations General Assembly resolutions calling for the protection of vulnerable marine ecosystems (VMEs), the Northwest Atlantic Fisheries Organization has closed 14 areas around the high-seas portion of Grand Bank and Flemish Cap to protect deep-sea coral and sponge habitats from impacts by bottom-contact fishing gears. Structural and functional connectivity for those areas were not explicitly considered in the area-selection process. We applied a particle-tracking model in each of four seasons to produce dispersal trajectories at the surface and 100 m from start points within the closed areas. These were run in forecast and hindcast modes to identify dispersal kernels. Currents at the surface, 100 m, 1000 m and "on bottom" were examined under an independent model (NEMO) to infer structural connectivity among the areas at relevant depths not available in the particle-tracking model. Spawning times and planktonic larval duration of the dominant sponges, sea pens and gorgonian corals were then considered to evaluate the trajectories as biophysical models, while species distribution models identified potential source populations from hindcast projections. Five of the 14 areas, including the three largest closures, showed particle retention, with three others showing retention within 10 km of their boundaries. The regional pattern of currents and their topographic forcing emerged as a strong structuring agent. A system of weakly-connected closed areas to protect sea pen VMEs on Flemish Cap was identified. The conducted approach illustrates the added value of assessing/modelling networking properties when designing MPAs.

1. Introduction

Connectivity is an emergent property of landscapes that influences the structure, biodiversity, productivity, dynamics and resilience of ecosystems (Baguette et al., 2013). It does so by providing feedbacks and subsidies of organisms, nutrients, and energy across ecosystem boundaries through both active and passive processes. Knowledge of population- and landscape-connectivity in marine systems is an important foundation for place-based conservation measures, such as marine protected areas (MPAs), and especially for the design of MPA networks (White et al., 2014; Gallego et al., 2017; Andrello et al., 2017). It is also necessary when evaluating the vulnerability of populations to environmental change and anthropogenic stressors. Further, the protection of connected networks can be a conservation objective of itself and has been advanced as a means of mitigating climate change impacts (Crooks and Sanjayan, 2006; Brock et al., 2012).

Connectivity theory in landscape ecology distinguishes between "structural connectivity" which is related purely to the physical environment and "functional connectivity" which is defined as the movement of adults, gametes or larvae across space, connecting populations and habitats (Hanski, 1998; Tischendorf and Fahrig, 2000). Effective connectivity further calls for successful settlement and survivorship of gametes or larvae while genetic connectivity (or "reproductive population connectivity") entails survivorship of settled larvae through to adult reproduction (Pineda et al., 2007).

Most marine ecosystems maintain strong functional connections through spatial fluxes (Lundberg and Moberg, 2003; Shanks et al., 2003; Pineda et al., 2007). However, little is known about connectivity in the deep sea in waters below 200 m. Technical difficulties have impeded research on larval biology and ecology of deep-sea benthic organisms and consequently the understanding of population connectivity in terms of deep-sea larval dispersal is a field still in its infancy (Young et al., 2012). For such species the pathways of larval dispersal can be predicted using simple biological parameters combined with physical

* Corresponding author.
E-mail address: Ellen.Kenchington@dfo-mpo.gc.ca (E. Kenchington).

https://doi.org/10.1016/j.dsr.2018.11.007
Received 24 May 2018; Received in revised form 3 October 2018; Accepted 19 November 2018
Available online 23 November 2018

Table 1
Characteristics of closed areas on Flemish Cap and Grand Bank. (Descriptors: FC = Flemish Cap; Conservation targets: S = Sponge grounds, SGC = Small gorgonian corals, LGC = Large gorgonian corals, SP = Sea pens (see Table 2 for more detail); Sources of Depth Data: MB = Multibeam bathymetric data from the NEREIDA program (https://www.nafo.int/About-us/International-Cooperation); CHS = Canadian Hydrographic Service 15″ resolution bathymetric data, derived from multiple sources including soundings).

Closed area number	Description	Conservation target(s)	Centroid position		Min. depth (m)	Mean depth (m)	Max. depth (m)	Depth data source	Surface area (km^2)
			North latitude (decimal degrees)	West longitude (decimal degrees)					
1	Tail of the Bank	S, SGC	44.20447608	48.82588955	1174	1516	1917	MB	143.8
2	Flemish Pass/ Eastern Canyons	S, LGC, SP	45.95552852	47.58203906	483	1262	2211	CHS	5421.4
3	Beothuk Knoll	S	45.90800000	46.20150000	921	1431	2598	MB	307.6
4	Eastern FC	S, LGC	46.89497763	43.60154624	567	1272	2754	CHS	1357.6
5	Northeast FC	S, LGC	48.19581916	43.87784885	938	1776	2688	CHS	2878.6
6	Sackville Spur	S	48.64756538	45.90851216	1224	1562	1952	MB	987.5
7	Northern FC	SP	48.37511469	45.08802952	590	650	718	CHS	258.0
8	Northern FC	SP	48.62748555	45.19051414	905	978	1088	MB	97.9
9	Northern FC	SP	48.53746623	45.55028338	876	992	1120	MB	127.7
10	Northwest FC	SP	47.96539095	46.19322300	1013	1127	1177	MB	315.6
11	Northwest FC	SP	47.46520000	46.40788889	910	1067	1132	MB	60.5
12	Northwest FC	SP	48.23559466	45.83344535	922	958	1003	MB	35.1
13	Beothuk Knoll	LGC	46.28964676	45.87214020	523	666	924	CHS	338.4
14	Eastern FC	SP	47.62918468	43.92847085	578	627	688	CHS	239.1

oceanographic models of the direction and speeds of currents (Young et al., 2012). While physical factors may not entirely constrain movements of active swimmers (e.g., fish, marine mammals, turtles), for sessile and sedentary animals that solely rely on larvae and asexual propagules for dispersal, they may be primary determinants of dispersal kernels (Cowen and Sponaugle, 2009; Young et al., 2012; Radice et al., 2016). Examples of physical factors that influence structural connectivity in the marine realm include currents, topographic forcing by bathymetric features, internal waves and tides, boundary layers, and water masses contributing to pycnoclines, haloclines, and thermoclines (Crooks and Sanjayan, 2006; Pineda et al., 2007).

In response to United Nations General Assembly (UNGA) resolutions calling for the protection of vulnerable marine ecosystems (VMEs), over the course of the past decade the Northwest Atlantic Fisheries Organization (NAFO) has closed 14 areas around the high-seas portion of Grand Bank and Flemish Cap (in addition to seamount closures and a transboundary closure with Canada) to protect deep-sea coral and sponge habitats from impacts by bottom-contact fishing gears (NAFO, 2017; Table 1; Fig. 1). The closed areas around Flemish Cap and Grand Bank (Table 1) vary in depth from 483 m to 2754 m, and are situated along different aspects of the banks, exposing them to different water masses and currents. The Labrador Current (Han, 2005), Gulf Stream (Fu et al., 1987) and North Atlantic Current (NAC) (Yaremchuk et al., 2001) are the dominant currents in the region. Structural and functional connectivity among those closed areas and with adjacent open areas were not considered in the area-selection process, although recognition of a "system" of closed areas to protect sea pens in the shallower waters of Flemish Cap was later advanced, inferred from their distributions (NAFO, 2013).

Herein, we examine structural connectivity among these 14 closed areas, with emphasis on connections between areas closed to protect the same taxa. To evaluate the potential for functional connections between areas given the poor knowledge of the reproductive and larval biology of the species of interest, we used a scenario-testing approach to run the models using a range of realistic parameters to evaluate potential dispersal kernels. Passive-particle dispersal was assessed using seasonal-modelled drift trajectories at two depths (surface and 100 m). To independently validate the passive-particle drift trajectories and importantly, to extend those results to the sea floor, currents at depth from an eddy-resolving model were investigated (the surface, 100 m, 1000 m and "on-bottom" depths). The realism of the modelled currents was validated with the observed surface currents from drifter data. In order to identify potential source populations we also ran the particle-tracking models in hindcast mode, and compared the points of origin with those of species distribution models of the probability of occurrence of the benthic taxa. Areas that are currently unprotected from bottom fishing that could be important for maintaining populations in the closed areas were so identified. We assessed the degree of structural connectivity among the closed areas, reviewed the scope for functional connections between areas with the same conservation targets, and considered management options to strengthen the achievement of their conservation objectives. For the latter we evaluated the existing closed areas against the marine protected area network ecological criteria put forward for the design of MPA networks to increase their conservation potential (WCPA/IUCN, 2007). To our knowledge this is the first examination of connectivity between areas closed by regional fisheries management organizations to protect VMEs in the high seas.

2. Materials and methods

2.1. Closed areas and oceanographic setting

The closed areas lie amidst a very complex topographic setting (Fig. 1C) which influences bottom current velocity. Flemish Cap is shallow, with a minimum depth of 125 m. It is separated from Grand Bank by the Flemish Pass, a mid-slope channel 1000 m deep (Piper and Campbell, 2005). The continental slope is very steep on the southern flank of the Cap, where the depth increases from 200 to 1000 m over a distance of 30 km; depth change is more gradual on the northern and eastern slopes (Gil et al., 2004). The continental slope to the southeast of Grand Bank is deeply incised with submarine canyons with steep depth gradients, while the slope to the northeast is much more gradual (Fig. 1).

A number of different water masses are found between the seabed and the surface waters, which have the potential to impede vertical migration of marine invertebrate larvae (Young et al., 1996a, 1996b, 2012; Crooks and Sanjayan, 2006; Shanks, 2009; Radice et al., 2016). Beneath the surface waters, which originate from shelf waters and Arctic outflows, are two kinds of intermediate waters: Subarctic Intermediate Water (SIW) and Labrador Sea Water (LSW). The former occupies the upper intermediate layer and is formed through mixing and subduction in the frontal zone, while the latter is typically found deeper in the water column and is known to be a product of winter convection in the Labrador Sea. Temperature and salinity of these waters have

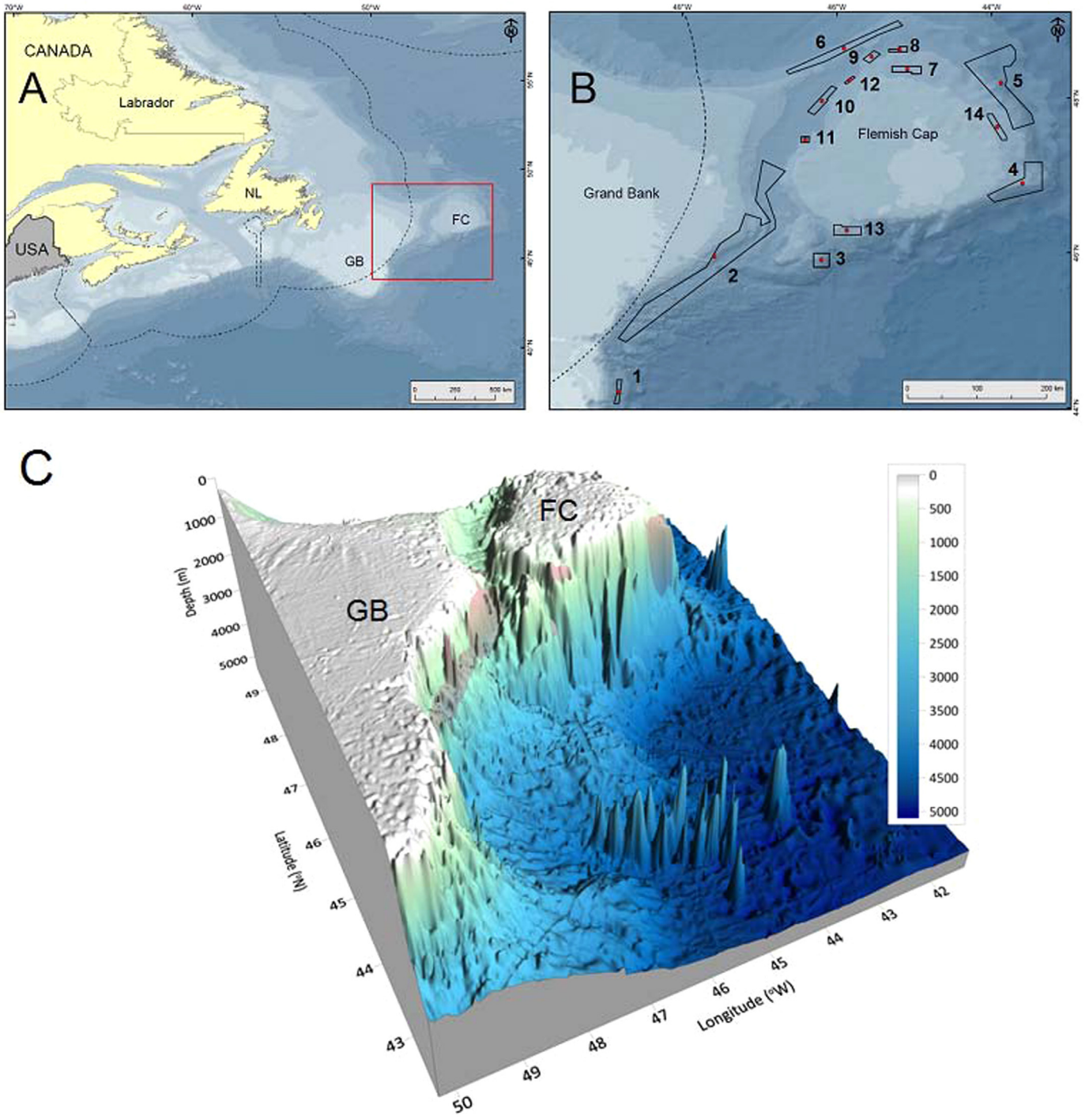

Fig. 1. Maps of the study region A) showing placement relative to Canada and the USA; B) close-up (red box on left panel) of the areas closed to bottom fishing activities by the Northwest Atlantic Fisheries Organization (NAFO) to protect sea pens, gorgonian corals and sponges considered herein; C) three dimensional representation of the study area (including seamount features). Numbers in B) refer to closed areas in the NAFO Conservation and Enforcement Measures for 2017 (NAFO, 2017) some of which are depicted by beige shading in C. Red circles in B) indicate the start positions for the forward drift trajectories (Table 1). Boundaries of national jurisdictions are indicated by dashed lines. NL = Newfoundland; GB = Grand Bank; FC = Flemish Cap.

shown significant variability on seasonal to decadal timescales (Schneider et al., 2015). Multiple cores of LSW ranging in density and depth (from 500 to 2500 m) have been mapped (Yashayaev, 2007; Yashayaev and Loder, 2016). LSW is underlain by two more water masses: Northeast Atlantic Deep Water (NEADW), originating from the Iceland-Scotland Overflow, and oxygen-rich Denmark Strait Overflow Water (DSOW). Those two water masses are important for understanding the complex oceanography of the region and supply of oxygen and nutrients to the benthic layer. The closed areas at depths exceeding 1700 m (Table 1) are likely to encounter NEADW, and below 2400 m, DSOW.

2.2. Biological traits and issues for parameterizing physical dispersal models

The closed areas host very different benthic assemblages composed of species of deep-sea sponges, sea pens or gorgonian corals (Table 2;

Table 2
Summary of knowledge on biological characteristics of dominant sponge, sea pen and coral species targeted for protection on Flemish Cap and the Tail of Grand Bank. UNK = Unknown or inconclusive evidence. See Sections 2.2.1 and 2.2.2 for more details.

Common name	Species	Spawning season	Literature reference	Planktonic larval duration	Literature reference
Sponges	All			< 2 weeks	Maldonado (2006)
	Geodia barretti	Summer, Autumn	Spetland et al. (2007)	UNK	
	Geodia phlegraei	July?	Cárdenas et al. (2013)	UNK	
	Geodia parva	UNK		UNK	
	Stelletta normani	UNK		UNK	
	Stryphnus fortis	UNK		UNK	
Sea Pens	*Anthoptilum grandiflorum*	April-July	Baillon et al. (2014)	UNK	
	Funiculina quadrangularis	Mid-winter	Edwards and Moore (2009)	UNK	
	Halipteris finmarchica	April-August	Baillon et al. (2015)	UNK	
	Pennatula aculeata	July-August (*P. phosphorea*)	Edwards and Moore (2008)	UNK	
Gorgonian Corals	*Paramuricea grandis*	June (*P. clavata*)	Coma et al. (1995)	Few minutes (*P. clavata*)	Coma et al. (1995)
	Paramuricea placomus	June (*P. clavata*)	Coma et al. (1995)	Few minutes (*P. clavata*)	Coma et al. (1995)
	Paragorgia arborea	UNK		UNK	
	Paragorgia johnsoni	UNK		UNK	
	Primnoa resedaeformis	2–3 peaks a year (*P. pacifica*)	Waller et al. (2014)	UNK	
	Keratoisis grayi	Late summer (as *K. ornata*)	Mercier and Hamel (2011)	UNK	

NAFO, 2013; Kenchington et al., 2014). Those taxa are sessile and therefore incapable of juvenile or adult movement, relying on transport of gametes and larvae to functionally connect across space to appropriate settlement sites, under the constraints imposed by structural connectivity features. Our particle tracking models (Section 2.3) allow for selection of three parameters which influence the particle trajectories. The values for those parameters were chosen through consideration of the known or predicted biological traits of the sponge and coral species under protection (Table 2). The biological traits are spawning season(s), position of gametes and larvae in the water column, and duration of larvae in the water column (planktonic larval duration, PLD), although Young et al. (2012) have modelled deep-sea larval dispersal using only PLD. For those taxa of conservation interest in the NAFO region, there is no specific information on PLD or position of larvae in the water column, whilst only minimal information is available on spawning season for some species (Table 2). Consequently, at this time, larval dispersal paths in this region can only be inferred from models evaluating structural connectivity under a range of realistic scenarios. However, we hypothesize that physical connectivity will be an important constraint on larval dispersal kernels in the NAFO region due to strong topographic forcing influencing the velocity of bottom currents. Sections 2.2.1 and 2.2.2 detail the rationale behind the selection of biological traits used in our dispersal models (Section 2.3.) for this study.

2.2.1. Sponges

Six of the 14 closed areas were put in place to protect sponge ground ecosystems (Table 1) formed by large structure-forming sponge species which host large numbers of associated fauna (Beazley et al., 2015). At depths of 700–1400 m on the eastern and southeastern slopes of Flemish Cap and Grand Bank, the sponge assemblage is typified by *Geodia barretti*, *G. parva, G. phlegraei*, *Stryphnus fortis*, and *Stelletta normani* (Murillo et al., 2016). Among those species, gametogenesis has been described only for *G. barretti* (Spetland et al., 2007). All five species belong to the same phylogenetic lineage, the Astrophorine Tetractinellida, and they are all suspected to be gonochoric and oviparous, with an external embryo development that remains undescribed and that theoretically should produce a free-swimming larval stage, which also has not been observed (Maldonado and Riesgo, 2008). In this general pattern, there may be an exception: the very atypical excavating sponges in the genera *Alectona* and *Thoosa*. They have affinities with the Astrophorine sponges (Maldonado, 2004; Borchiellini et al., 2004) and produce a brooded larval stage, the hoplitomella (Garrone, 1974; Vacelet, 1999; Maldonado and Bergquist, 2002; Bautista-Guerrero et al., 2010). A peculiarity of the hoplitomella is that, unlike all other known sponge larvae, it lacks cilia for active locomotion. The larva is also peculiar because it develops a distinct skeleton of siliceous spicules, some of them projecting radially out of the larval body, giving the larva a radiolarian-like aspect. As in the case of radiolarians, these protruding spicules operate as floating devices that increase drag by augmenting the surface area of the larval body, preventing in turn sinking by the effect that the viscose forces of seawater exert on the tiny larval body (see Young, 1995; Maldonado, 2006 for a review of mechanisms). This functional design has made the hoplitomella to be the only sponge larva that consistently appears in samples of offshore plankton (Trégouboff, 1939, 1942), despite being the only sponge larva lacking cilia for active swimming. It is also the sponge larva hypothesized to live for extended periods (may be months) in the water column (Maldonado, 2006). All known sponge larvae are lecithotrophic, which means that they cannot incorporate external food (unlike planktotrophic larvae) and that the energy required for dispersal is basically supplied by the stored yolk. Because of this energetic constraint, lecithotrophic larvae have typically shorter dispersal periods than planktotrophic larvae, which for most known shallow-water sponge species ranges from a few minutes to about two weeks (Maldonado, 2006). Only the hoplitomella is suspected to remain in the plankton for longer periods (Trégouboff, 1939, 1942). Since the larval stage of Astrophorine sponges has never been seen, we cannot discard the possibility that it may not be one of the typical short-lived, ciliated forms, but rather a larval stage similar to the hoplitomella and adapted to drift in the water column longer than the mere 2-week period estimated for most parenchymella larvae. Interestingly, the dispersal stage known in Spirophorine sponges (which form the sister lineage of Astrophorine sponges) is another unciliated form characterized by bearing protruding spicules (Watanabe, 1978; Maldonado et al., 2017), although it is considered to be an embryo that experiences direct development rather than through a larval stage (Maldonado and Bergquist, 2002). All together and despite the many unknowns for the larval stage of the dominant sponges in the closed areas, the available information advise that, if we are to model sponge larval dispersal, several different planktonic dispersal periods (2 weeks, 1 month, and 3 months) should be considered to encompass all potential scenarios.

The season of release is also a relevant factor in modelling particle dispersal. But, again, the information for the concerned sponge species is very scarce when selecting the timing for gamete release. The timing of gametogenesis is available only for *Geodia barretti* (Spetland et al., 2007). This information derives from populations very distant from the ones in the concerned closed areas, being located on the eastern side of the Atlantic Ocean and established on the deep continental shelf (60–250 m) in Norwegian fjords rather than at bathyal depths. In those studies, one (Spring) or two (Spring and Autumn) discrete peaks of gamete release were identified over the year cycle (Spetland et al.,

2007). In both cases, gamete maturation appeared to be synchronized by pulses of particulate food arriving to the bottom after seasonal blooms of phytoplankton in the superficial layers. Similar pulses of sinking primary production have also been suggested to synchronize reproduction in other deep-shelf and deep-sea sponge assemblages (Witte, 1996; Maldonado et al., 2017). Because of a lack of information for the concerned species in the closed areas, biological inferences from our models will assume gametogenic timing similar to that described for *G. barretti*, incorporating both a spring and autumn period of larval production. Yet, we are aware there are precedents for shallow-water sponges indicating that reproductive timing may vary among distant populations, as demonstrated by Hawaiian populations of the haplosclerid demosponge *Halichondria melanodocia* releasing larvae in February and the Floridian populations doing so in April (Woollacott, 1990).

The behavioral capability for horizontal active swimming and vertical displacement in the water column are also biological parameters that can be factored into particle dispersal models. The maximum horizontal speed measured in displacements of sponge larvae to date is about 1 cm s^{-1}. However, that speed reflects an extreme laboratory behavior developed as an escape reaction by a photonegative parenchymella when exposed to bright light (Maldonado and Young, 1996). Scuba-diving observations of free swimming larva of shallow-water sponges in natural conditions have revealed that, most of the time, larvae do not displace horizontally by active swimming. Rather they "rest" in "vertical position", rotating along their long axis while drifting passively with water current, as "balloons" trapped by the viscose forces of seawater (Maldonado, 2006). Therefore, in terms of horizontal locomotion, sponge larvae can reliably be modelled as passive particles. However, they may have the capability to migrate vertically to pick different water masses for dispersal. Studies on shallow-water sponges have shown that larvae of some species are initially photopositive and full of lipids, two features that would help larvae to ascend from the bottom to the water column and select horizontal currents for a more effective dispersal. For such larvae, at the time of settlement, they became photonegative and lose buoyancy, helping them to find the bottom (Maldonado, 2006). Many deep-sea invertebrate larvae display a similar pattern of ontogenetic vertical migration because the dispersal in surface waters should be greater than that in the slower currents of the deep sea (Young, 1995; Young et al., 1996a, 1996b). Whether special mechanisms operate in deep-sea sponges to successfully perform long vertical migration is completely unknown. The occurrence of hoplitomella larvae in off-shore seawater samples aimed to collect phytoplankton (Trégouboff, 1939, 1942) strongly suggests that, at least, this kind of larvae can ascend from the deepest bottoms of the continental shelf. However, the other kinds of sponge larvae are very rarely found in such offshore samples and the use of plankton nets or scuba divers to sample at short distances above the sponge bottoms has revealed that large quantities of larvae actually remain in the demersal water layer close to the parental habitat (Mariani et al., 2005, 2006). Here we have modelled dispersal at the surface and at 100 m, but also examined how the general patterns of the currents are maintained within depth at 1000 m and the sea floor and interpreted dispersal trajectories mindful of the comparatively decreased velocities registered at the bottom.

2.2.2. Cold water corals

Eleven of the 14 closed areas offer protection to cold water corals from bottom contact fishing gears, with Areas 7–12 and 14 closed primarily to protect sea pen fields and Area 13 to protect large gorgonian corals (Table 1; NAFO, 2013). Octocorals, including sea pens and gorgonian corals, have two modes of sexual reproduction: 1) broadcast spawning and external fertilization of gametes, and 2) internal fertilization and brooding of planula larvae (Kahng et al., 2011). Brooders may develop larvae internally, or attached to the external surface of the female colony; some produce crawling larvae which settle near the parent colony.

Anthoptilum grandiflorum, *Halipteris finmarchica* and *Pennatula aculeata* are the dominant sea pen species in the study area (Murillo et al., 2010), and these, along with *Funiculina quadrangularis* form a distinct community on sandy and clay-silt bottoms between 800 and 1200 m depth (Murillo et al., 2016). The reproductive biology of sea pens has been described for a few species. All are gonochoric and appear to be broadcast spawners (Chia and Crawford, 1973; Tyler et al., 1995; Soong, 2005; Edwards and Moore, 2008; Pires et al., 2009; Baillon et al., 2014, 2015), with large lecithotrophic larvae (Chia and Crawford, 1973; Edwards and Moore, 2008, 2009). *Anthoptilum grandiflorum* and *Halipteris finmarchica* have an annual spawning periodicity (Baillon et al., 2014, 2015); whereas *Pennatula aculeata* may be a continuous spawner (Eckelbarger et al., 1998) although it's congener *P. phosphorea* spawns in summer (Edwards and Moore, 2008). Nothing is known of the vertical position and PLD of sea pen larvae (Table 2) although their large lecithotrophic larvae may indicate short dispersal periods as seen in some sponges (Section 2.2.1, Maldonado, 2006).

Areas 2, 4, 5 and 13 were closed to protect large gorgonian corals. These corals are primarily *Paragorgia arborea*, *P. johnsoni*, *Paramuricea grandis*, *P. placomus, Primnoa resedaeformis*, and *Keratosis grayi* (Murillo et al., 2011, 2016), although other cryptic species of *Paramuricea* not yet described could also be present (Radice et al., 2016). The reproductive biology of some of these coral species, or their congeners, has been studied providing some indication of spawning season (Table 2). *Paramuricea clavata*, a shallow-water Mediterranean congener of *P. grandis* and *P. placomus*, is an external brooder that spawns at the end of May, with embryos developing adhered to the surface of the female colony, and short-lived larvae typically settling at the base of the female parent and on the surrounding substrate within minutes after hatching (Coma et al., 1995). It is unknown whether the deep-water species of *Paramuricea* occurring in the study area also produce such short-lived larvae. The bamboo coral *Keratoisis grayi* is a broadcast spawner, spawning in late summer (Mercier and Hamel, 2011; as *K. ornata*). The Alaskan populations of *Primnoa pacifica*, a congener of *P. resedaeformis*, are gonochoric broadcasters, with a gametic maturation as long as a year, and apparently with several events (2 or 3 peaks) of gamete release in the population over a year cycle; the species is suspected to develop a lecithotrophic larva (Waller et al., 2014). *Paragorgia arborea* is suspected to be one of the few brooders in its group (Lacharité and Metaxas, 2013), while *Paragorgia johnsoni* and *Primnoa resedaeformis* are believed to be broadcast spawners (Mercier and Hamel, 2011), but in all cases spawning seasons and planktonic larval durations are undocumented. Mercier and Hamel (2011) suggest that *P. resedaeformis* and *K. grayi* have non-feeding larval modes, which theoretically imply short larval durations and perhaps deeper drift depths. Yet, there are plenty of examples of lecithotrophic marine invertebrate larvae with long planktonic life that may extend from one to 17 months, particularly among asteroids and holothurians (Grant, 1983; Pearse, 1994; Hadfield and Strathmann, 1996). Examples of long lecithotrophic larval life also include planulae of alcyonacean soft corals, which may have competency periods over two and three months, facilitating long distance transport (Ben-David-Zaslow and Benayahu, 1996, 1998; Dahan and Benayahu, 1998). Despite the above pieces of indirect evidence, as for the sea pens, the PLD and position of larvae in the water column for the relevant gorgonian octocorals of the protected areas remain undocumented (Table 2). Thus, our assumptions for drawing biological inferences from our modelling have been derived from the scarce indirect evidence that is available.

2.3. Passive-particle drift trajectories

There are a number of passive-particle tracking models available, many of which use flow fields from a particular ocean model, coupled with a tracking algorithm (Fredj et al., 2016). Here we used the Web-drogue Drift Prediction Model v.0.7, together with the “Southern

Labrador, Newfoundland Shelf" data set (http://www.bio.gc.ca/science/research-recherche/ocean/webdrogue/slns-tnls-en.php accessed 23 May 2018). Webdrogue draws on regional historical observations and primitive-equation numerical models with forcing by tides, wind stress, and baroclinic and barotropic pressure gradients and was developed as an offline tool by Fisheries and Oceans, Canada. The model incorporates several tidal/inertial periods to bring the temperature, salinity, density, turbulence, elevation, and velocity fields into a quasi-steady dynamical balance (Hannah et al., 2000). Webdrogue uses climatological currents but does not reflect random velocity perturbations and so does not account for stochastic events which could influence larval dispersal. Details of the computation of the wind-driven circulation and the combination of the circulation components are provided by Hannah et al. (2000) and those of regional data sources by Han et al. (2008). The resolution of the model is high on the Flemish Cap and on the shelf break with a typical nodal spacing of ~ 5 km. The predictive model was run for each of four, two-month seasons available in Webdrogue: Winter (January, February), Spring (April, May), Summer (July, August), and Autumn (October, November), to obtain their seasonal fields. Within each of those seasons any starting date and duration can be chosen, however depth is fixed and only three depth selections can be utilized (surface (2.5 m), 25 m, 100 m) with this program.

The initial start positions for the drift trajectories were the centroids of each of the 14 closed area polygons (Table 1, Fig. 1), determined using the "Feature to Point" tool in ArcGIS 10.2.2 software (Redlands, California, USA). Particle release dates were the mid-point of each season (i.e., the first of February, May, August and November), after preliminary runs showed that there was no large difference in the trajectories produced from start dates earlier or later within the two month seasonal windows. Predictions were run using 60 min time steps at each of two depths, "surface" (2.5 m) and 100 m. The predictions were run for durations of 2 weeks, 1 month, and 3 months – the latter to determine dispersal kernels and identify gyres, although three months is likely an unrealistically long larval duration for most coral and sponge species in this region (Sections 2.2.1. and 2.2.2.).

Particle trajectories were non-linear and so our results are not presented as distances travelled. Instead the locations of the predicted endpoints, relative to the closed area boundaries and 2 km and 10 km buffers around those boundaries (to account for the ~ 5 km resolution of the model in this region), as well as to the larger areas described as VMEs by NAFO (2013) (hindcast mode only), were determined using the "Spatial Join" tool in ArcMap within the ArcGIS Desktop. These areas were selected to address specific management-related questions regarding the size of the current closed areas and to acknowledge the resolution of the prediction model (i.e., 2 km from a boundary could not be distinguished from "inside" the closed area boundary, and 10 km was likely outside but close to the boundary). We further focussed on interpreting bio-physical connectivity between and among closed areas that were closed to protect the same conservation targets (Table 1).

In addition to those trajectories from closed area centroids, we modelled particles initiated from 50 randomly-chosen start positions within the closed areas to examine variation in the end points, and to identify connectivity between portions of the larger closed areas that were inadequately represented by their area centroids. As those trajectories were highly consistent with that of the centroid position, the latter was used to display dispersal kernels in associated figures.

2.3.1. Independent validation of particle tracking models and calculation of flow fields to 1000 m and the sea floor

To construct an independent validation of the Webdrogue particle tracking trajectories which were based on regional observations and models, we compared our results with those produced by a general model of ocean circulation developed by a European consortium and with Lagrangian drifter data from satellite-tracked drifting buoys. For the first approach, currents were computed using an eddy-resolving model based on NEMO (Nucleus for European Modelling of the Ocean) version 2.3, as applied by Wang et al. (2016). The model domain included the North Atlantic Ocean with a nominal resolution of 1/12° (~ 5 km in the study area). Averaged currents over the 1990–2015 period at the surface, 100 m, 1000 m and on-bottom were plotted. The surface and 100 m depth plots were compared with the passive-particle drift model solutions produced by Webdrogue, while the 1000 m and on-bottom depths were used to evaluate the effect of increasing depth on those trajectories.

The NEMO-derived model is layered, the thickness of each layer varying from 1 m at the surface to 100 m at a depth of 1250 m and a maximum value of 460 m at the bottom of the deep basins (5730 m). In this study, the current from the lowest layer above the seabed was used to represent the on-bottom current, though the distance between the vertical location of the layer and the real seabed was variable, generally increasing with water depth. To address this, we employed a partial-cell technique to depict the ocean water depth, which greatly decreased the maximum layer thickness (from 100 m to approximately 20 m at 1250 m depth).

Model outputs were further compared with sea-surface observational data to evaluate model performance. We used Lagrangian drifter data from satellite-tracked drifting buoys from 1990–2015 (obtained from the Drifter Data Assembly Center (DAC) at NOAA's Atlantic Oceanographic and Meteorological Laboratory (AOML) under the Global Drifter Program (http://www.aoml.noaa.gov/envids/gld/ accessed 23 May 2018)). Along-track satellite altimeter data from 1993 to 2015 were obtained through Archiving, Validation and Interpretation of Satellite Oceanographic (AVISO) data; https://www.aviso.altimetry.fr/en/data/data-access.html accessed 23 May 2018) and used to calculate the root-mean-squared sea surface height as an estimate of variability of surface currents.

2.4. Species distribution models

Random Forest (RF) models (Breiman, 2001) of presence probability, "species distributions models" (SDMs), based on the presence/absence of sponges, sea pens and large gorgonian corals were generated for the NAFO Regulatory Area on Grand Bank and Flemish Cap. RF is a non-parametric machine learning technique that in general provides better performance when compared with other methods for predicting species' distribution (e.g., Alabia et al., 2016). The spatial extent for the analysis was the NAFO "fishing footprint", the deep margin of which closely follows the 2000 m depth contour (NAFO, 2017). The models were built in R 3.5.1 (R Core Team, 2018) using the "randomForest" package (Liaw and Wiener, 2002) with default values for RF parameters and generation of 500 trees from random subsets of the data. Details of model application followed Guijarro et al. (2016a), who used similar methods to model species distributions in adjacent Canadian waters.

Response data, on the presence and absence of functional groups, i.e., sponges, sea pens and large gorgonian corals, were drawn from European Union (EU)-Spanish and Canadian DFO-Newfoundland and Labrador research vessel bottom-trawl surveys conducted in the NAFO Regulatory Area (survey details in Knudby et al., 2013a and Kenchington et al., 2014). Null data were only considered when presence records of the same taxon were made on the same survey, to avoid including false negatives. Knudby et al. (2013b) performed RF models of sponge grounds. We chose to additionally model the presence probability of all sponges (Porifera) on the basis that species compositions are not fully documented and effective recruitment could originate from only a few sponges living outside of the sponge ground habitats.

For sponges the data were from 2006 to 2016 from surveys conducted by EU-Spain and from 2005 to 2015 from Canadian surveys, and included all records of sponges. The total number of such records was 5178, including 2910 presences. For sea pens and large gorgonian corals, EU-Spanish data were available for 2005–2016. The total

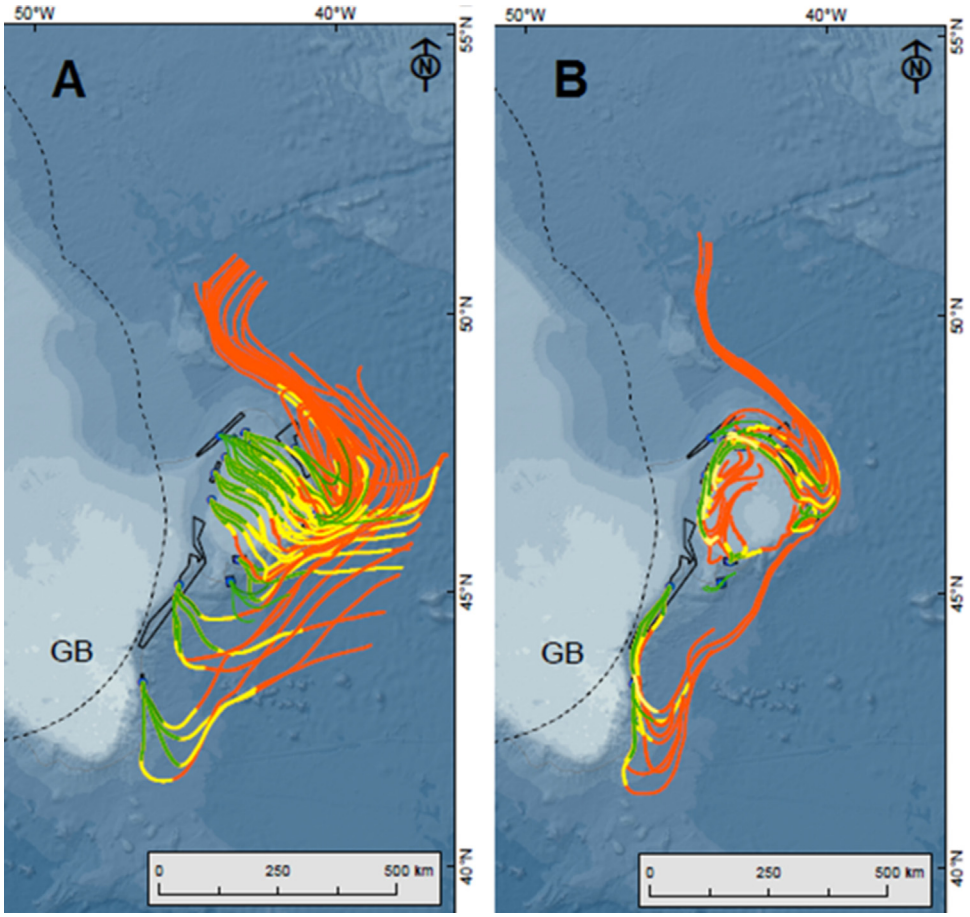

Fig. 2. Passive particle drift trajectories from the centroids of each of the 14 closed areas in each of four seasons (not differentiated with colours but trajecting from the same origin in each closed area). Duration times of 2 weeks (green), 1 month (yellow) and 3 months (orange) are shown for A) Surface waters, and B) Drift at 100 m depth. Dashed line indicates the boundary of Canadian jurisdiction. GB = Grand Bank.

number of sea pen records was 4593, with 1622 being presences. For large gorgonians, the trawl-survey data were augmented by photographic transects and rock dredge samples reported in Knudby et al. (2013a), as those corals can occur on rough bottoms avoided by the trawl surveys. The total number of large gorgonian coral records was 4132, including 241 presences.

The environmental predictor variables were the same 66 used by Guijarro et al. (2016b). They were selected based on their availability and assumed relevance to the distribution of benthic fauna and included seasonal minimums, maximums, ranges and averages where applicable. Each predictor variable was spatially interpolated across the study area using ordinary kriging in ArcMap (Guijarro et al., 2016b).

We used both balanced and unbalanced RF models without *a priori* variable elimination and chose the best performing model to represent the species distributions, model performance being evaluated by a 10-fold cross validation. Balanced designs were achieved through random down-sampling to remove absences. Three measures of accuracy were used to assess model performance: sensitivity, specificity, and Area Under the receiver operating characteristic Curve (AUC), in addition to visual examination of raw and modelled spatial data.

2.5. Hindcasting to identify source populations

Potential source populations for each of the 14 closed areas were investigated through hindcasting of particle-drift trajectories with Webdrogue, for the same depths, seasons and durations as used in the predictive trajectories, except for Area 6 and Area 3. Those were closed to protect only the sponge grounds (Table 1), and so only 2 week drifts were hindcast, reflecting the presumed short larval duration of that taxon (Section 2.2.1; Maldonado, 2006; Van Soest et al., 2012).

In addition to those hindcasts from closed area centroids, we hindcast particles initiated from 50 randomly-chosen start positions within the closed areas to examine variation in the end points, and to identify connectivity between portions of the larger closed areas that were inadequately represented by their area centroids.

The probabilities of occurrence of the taxa for which each closed area was established, based on our SDMs and for sponge grounds that of Knudby et al. (2013b), at the hindcast end points were extracted with the “Spatial Join” tool in ArcMAP. The entireties of the trajectories were visually compared with the SDMs. As noted in Section 2.3, areas described as VMEs by NAFO (2013) were examined to determine whether fished areas surrounding the closed areas could be important sources of recruitment.

2.6. Overlying oceanic water masses

Regional seawater-property maps were developed for standard oceanographic depths using temperature and salinity observations from 1930 to 2000 for the high-seas portion of Grand Bank and for Flemish Cap. The observed profile data were drawn from the Department of Fisheries and Oceans, Canada archive at the Bedford Institute of Oceanography, the collection of Soviet "Sections" Program oceanographic data (Yashayaev, 2000), the World Ocean Circulation Experiment archive, and the World Ocean Database maintained by the National Oceanic and Atmospheric Administration's National Oceanographic Data Center (NODC).

To achieve high spatial resolution (~ 35 km) of climatological metrics, including resolving climatic features at that scale, while reducing the effects of meso-scale eddies and meanders on the final property maps, the adaptive gridding algorithm of Yashayaev and Seidov (2015) and Yashayaev and Loder (2016) was followed. It was adjusted to the spatial density of historical observations (high over continental slopes

Table 3
Drift trajectories from closed area centroids that end within or near another closed area. (Bold: indicates connection between closed areas with the same conservation target and so potential paths of effective functional connectivity).

Drift depth	Drift duration	Season Spring	Summer	Autumn	Winter
Endpoint within another closed area					
Surface	2 weeks				Area 7 to Area 4
100 m	2 weeks		Area 8 to Area 5		**Area 9 to Area 8**
100 m	1 month		Area 9 to Area 5	Area 4 to Area 14	Area 8 to Area 5
100 m	3 months	Area 7 to Area 5			
100 m	3 months	Area 9 to Area 5			
100 m	3 months	**Area 12 to Area 7**			
Endpoint within 2 km of another closed area					
Surface	2 weeks	Area 8 to Area 5	**Area 8 to Area 14**		
100 m	2 weeks			**Area 9 to Area 10**	
100 m	1 month			**Area 14 to Area 9**	
100 m	3 months		**Area 10 to Area 14**		
Endpoint within 10 km of another closed area					
Surface	2 weeks				Area 8 to Area 4
Surface	2 weeks				Area 12 to Area 4
Surface	1 month	**Area 9 to Area 14**	Area 9 to Area 4		
Surface	1 month	Area 8 to Area 4			
Surface	3 months			Area 12 to Area 4	
100 m	2 weeks		**Area 12 to Area 7**		
100 m	2 weeks		**Area 12 to Area 10**		
100 m	1 month				**Area 7 to Area 8**
100 m	3 months				**Area 12 to Area 7**

and shelves) and by applying additional weights to the measurements based on their closeness to typical or modal conditions at each grid point. Those and other key steps of derivation of regional climatological conditions were implemented through recursive iterations, producing a set of optimal fields. General distributions of the main sub-surface and intermediate water masses overlying the closed areas were depicted in representative horizontal property maps covering the study area at 100 m, 1000 m and 1500 m depths.

3. Results

3.1. Passive-particle drift trajectories

Passive-particle drift trajectories from most area centroids showed advection out of the system; the particles being lost to the North Atlantic Current. This was observed at the surface and at 100 m depth, and with durations of 2 weeks or longer, in any of the four seasons (Fig. 2). The only exceptions were some trajectories at 100 m depth that were confined over Flemish Cap (Fig. 2B, Tables 3, 4) and some at the surface which crossed the Cap but did not escape from it (Fig. 2A, Table 3).

Collectively, 17 unique connection paths were identified across endpoint positions (to within another closed area and within 2 km and 10 km of another closed area), nine of which connected areas closed to protect the same conservation targets (Table 3). Nine seasonal connections, eight at 100 m depth and one at the surface, were identified from the centroid of one closed area to within the boundaries of another (Table 3). Seven of these were unique connections, across all seasons, while only two seasonal connections (both unique combinations) linked areas closed to protect the same taxon, both of which linked sea pen closed areas on Flemish Cap. Five of the nine seasonal connections linked from one closed area to Area 5, the largest of the closed areas on Flemish Cap. A sixth linked to Area 4, the second largest closed area there. Five other trajectories, two at the surface and three at 100 m, ended within 2 km of a closed area (and so not distinguishable from within the closed area given the resolution of the model) other than the one from which they started (four being new connections not recorded when considering only full connections from one area to another and all connecting the areas with the same conservation target – sea pens). An additional ten trajectories ended within 10 km of another closed area, six of which were new connections (Table 3). Nine of those 10 connections were between areas protecting the same taxa, all of them being sea pen areas on the Cap and therefore may represent potential paths of effective functional connectivity. Six of the connections created when considering the 10 km buffer were surface-surface connections only, one of which connected areas closed to protect the same conservation target, while the remaining four connections at 100 m depth all connected areas closed to protect sea pens (Table 3).

Table 4
Drift trajectories from closed area centroids that end within or near initial closed area.

Drift depth	Drift duration	Season Spring	Summer	Autumn	Winter
Endpoint within closed area					
100 m	2 weeks	Areas 2, 3, 4, 13		Area 5	Area 4
100 m	1 month	Area 4			
100 m	3 months				Area 4
Endpoint within 2 km of closed area					
100 m	1 month	Area 13		Area 5	
100 m	3 months	Area 4			
Endpoint within 10 km of closed area					
100 m	2 weeks	Areas 5, 9	Areas 13, 11		Area 14
100 m	1 month		Area 2		Area 4

In five of the 14 closed areas, the modelled drift trajectories at 100 m depth showed potential for particles to return to, or stay within, their initial closed area, primarily the large Areas 2, 4 and 5, and mostly in spring (Table 4). Particle retention was not observed in surface models.

3.1.1. Independent validation of particle tracking models and calculation of flow fields to 1000 m and the sea floor

Surface currents, as indicated by both drifters and climatological modelling, showed weak anti-cyclonic flows within the 500 m bathymetric contour on Flemish Cap, diminishing to the southwest (Fig. 3). Surface waters overlying seabed depths between 500 and 2000 m, where most of the areas closed to protect vulnerable marine ecosystems lie, had greater velocities and showed the expected bifurcation of the Labrador Current, with the strongest flows moving southwards through

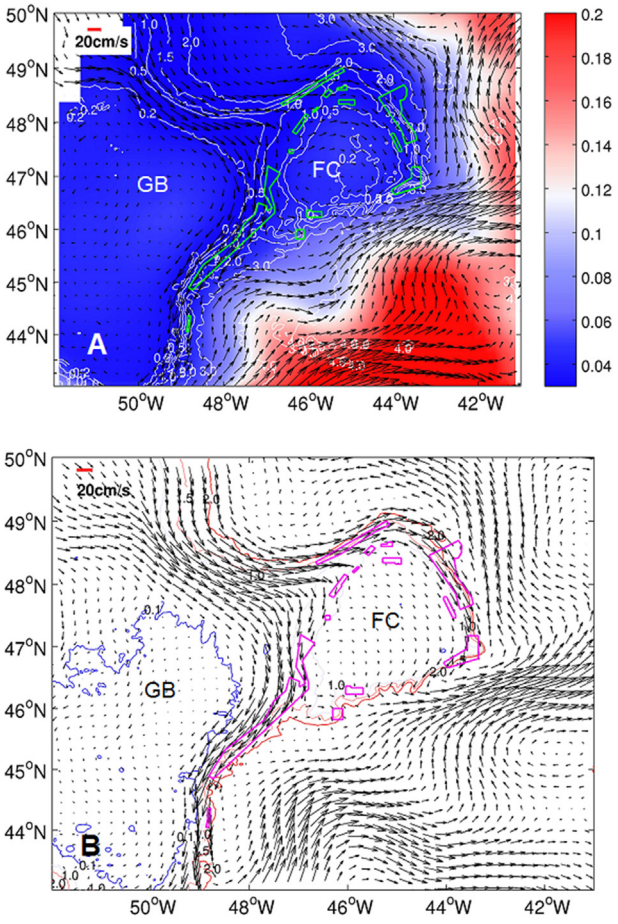

Fig. 3. Surface current flows. A) averaged surface currents (cm s^{-1}; legend upper left corner) from drifters, and sea-level variability (root-mean-squared sea surface height (m) from the satellite altimeter data (colour scale)); B) modelled surface currents based on NEMO (cm s^{-1}; legend upper left corner). For both plots, depth contours (km) and closed areas are depicted (A: green outline, B: pink outline). GB = Grand Bank; FC = Flemish Cap. Every third vector was plotted to avoid crowding.

Flemish Pass and weaker ones rounding Flemish Cap. The latter reverse direction south and east of the Cap, where they joined the North Atlantic Current (NAC). The altimeter data showed low variability (RMS) in sea surface height over Flemish Cap and Grand Bank (Fig. 3A). Higher variability to the east is associated with Gulf Stream meanders and eddies.

The drift trajectories produced using Webdrogue were consistent with the current flows calculated from the NEMO model, for both the surface and 100 m depth, and also with drift buoy observations (Fig. 3). The general pattern of the sub-surface currents are similar, though velocity decreases with depth in most areas, likely reducing the number of connections between closed areas from those observed at 100 m, while increasing the potential for retention (Fig. 4). One exception is the current flowing along the southern flank of Flemish Cap, which is stronger over greater distances at 1000 m than at the surface or 100 m, favouring a connection between deep-lying Areas 4 and 13. That increase in velocity mainly results from the influence of the NAC, which meanders towards the northeast with strong eddy activity, weakening the near-surface Labrador Current. At greater depth, topographic steering dominates, allowing the Labrador Current to follow f/H contours (f: Coriolis parameter; H: water depth). On the northern flank of Flemish Cap the current was equally strong at all three off-bottom depths (Figs. 3 and 4).

The modelled on-bottom currents (Fig. 5) showed strongest flows over the deep northern and eastern slopes of Flemish Cap, crossing Areas 6, 5 and 4. Velocities through the Flemish Pass were weaker and there was little to no current over Areas 7–14, on the top of Flemish Cap (Fig. 5).

3.2. Species distribution models

All species distribution models were best represented using unbalanced designs, as those gave the best fit to the data. Both balanced and unbalanced models produced similar maps of spatial distributions in all instances. In unbalanced models, species' prevalences were used to estimate absolute (rather than relative) probability of presence. Values below the prevalence threshold, here observation prevalence, indicate absence and those above, absolute probability of presence (Phillips and Elith, 2013).

The maps generated by our sea pen and large gorgonian coral SDMs, used for identifying potential recruitment sources, were consistent with those produced for the region previously (Knudby et al., 2013a). Our map of sponge distribution differed from that of sponge grounds (areas of high biomass) prepared by Knudby et al. (2013b), as expected. We therefore utilized both in our evaluations.

The average AUC for the sponge SDMs was 0.839 (± 0.015 standard deviation). The class errors of the presence and absence classes from the best fit model were 0.220 and 0.247 respectively, implying similar commission and omission error rates. The predicted relative probability surface for sponge presence is shown in Fig. 6. Prevalence was 56%. Sponges are predicted to occur through most of the region except for the shallow shelf areas on the Tail of Grand Bank (Fig. 6). The average annual range in sea surface temperature was the most important predictor variable.

For the SDMs run for sea pens, average AUC was 0.893 (± 0.021 standard deviation). The class errors of the presence and absence classes for the best fit model were 0.183 and 0.190 respectively. The predicted relative probability surface for sea pen presence is shown in Fig. 7. Prevalence was 35%. Sea pens are predicted to occur around the western, northern and eastern slopes of Flemish Cap, and in the deeper slope areas on the Tail of Grand Bank. The two most important predictors of sea pen presence were average annual minimum bottom salinity and depth.

The average AUC for the SDMs run for large gorgonian corals was (0.865 ± 0.038 standard deviation). The class errors of the presence and absence classes were 0.245 and 0.165 respectively, meaning higher commission than omission error. This favours a representation of species presence through a higher false positive rate, creating an appearance of greater potential habitat area (Roberts et al., 2011). The predicted relative probability surface of large gorgonian presence is shown in Fig. 8. Prevalence was 6%. Large gorgonian coral species are predicted to occur along the slopes of Flemish Cap and on Beothuk Knoll but to be absent elsewhere. Mean bottom salinity was much the most important predictor of large gorgonian coral presence.

3.3. Hindcasting to identify source populations

3.3.1. Areas closed to protect sponges

Hindcast passive-particle drifts, over 2-week durations at 100 m depth and leading to the centroids of areas closed to protect sponges, mostly originated in locations with a high probability of sponge occurrence (average 81% and minimum 55%, compared to the prevalence threshold of 56%: Table 5, Fig. 9). However, the sponges are widespread over the study area (Fig. 6) while dense aggregations, known as sponge grounds, are more common in the deeper slope waters (Murillo et al., 2012; Knudby et al., 2013b). The species composition in the sponge grounds differs from those over the whole of Flemish Cap (Murillo et al., 2016) and potential sources emanating from sponge grounds are likely more relevant to this application as the closed areas were put in place to protect sponge grounds. In most cases, those points of origin had much lower probabilities, 29% on average, of coming

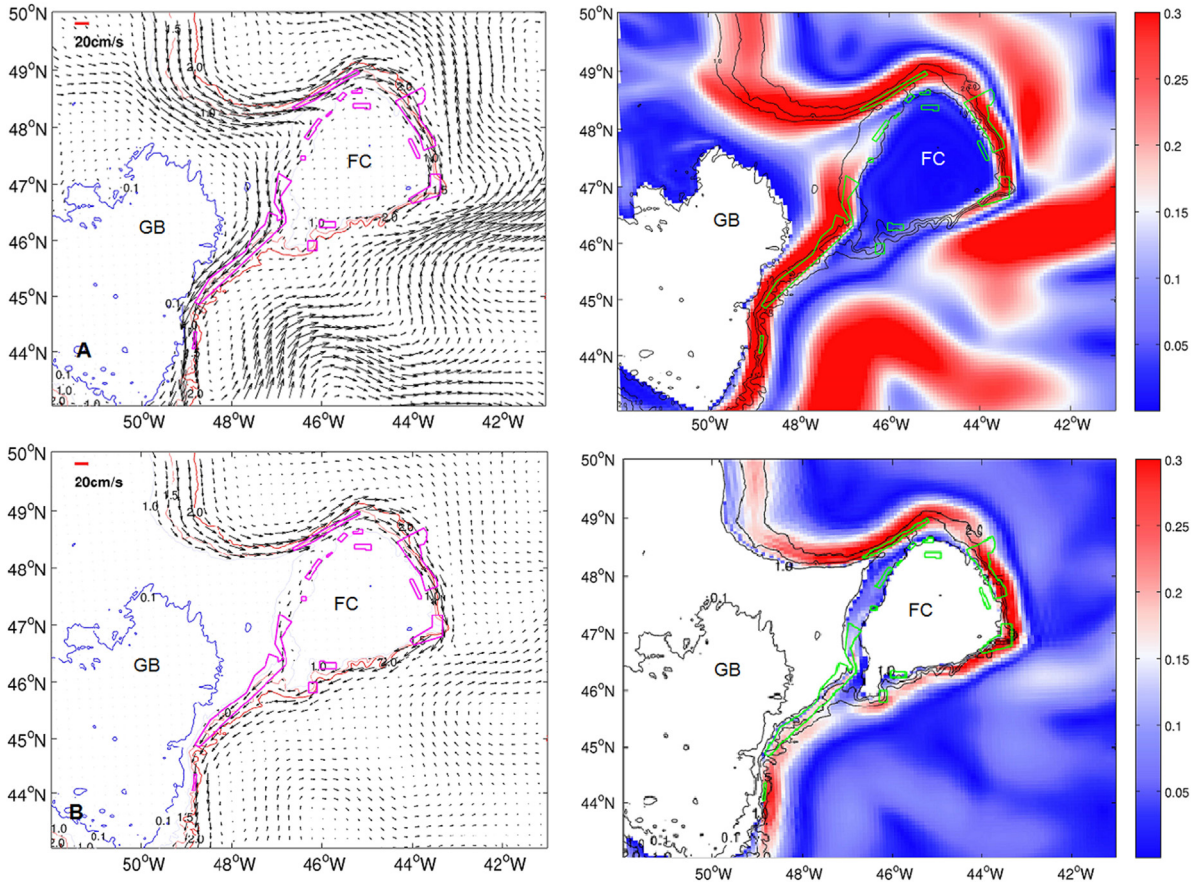

Fig. 4. Modelled currents (left panel) and current speeds (m/s; right panel) at A) 100 m and B) 1000 m depth (scale bar left corner). Depth contours (km $\times 10^3$) and areas closed by NAFO to protect VMEs (purple or green outline) are shown. Every third vector was plotted to avoid crowding. GB = Grand Bank; FC = Flemish Cap.

from "sponge grounds" identified as such by Knudby et al. (2013b). However, the drifts to Area 4 in the spring and winter, and to Area 1 in the summer, originated from locations that had very high probability of being sponge grounds (Table 5). Fifteen of the 24 equivalent surface drifts originated from outside the study area. All of the remaining nine had sources where the probability of sponge occurrence was below the prevalence threshold.

Hindcasting drifts to multiple points within the closed areas did not much alter those results, which was also true for sea pens and large gorgonian corals, probably because topographic forcing aligns the currents at 100 m depth with the bottom contours (Fig. 4). For sponges, the hindcast drifts suggested a potential for the sponges in Area 2 to draw recruitment from the Nose of Grand Bank, and those in Area 6 from the continental slope to the west (Fig. 9). The hindcasts leading to multiple points also revealed a link from the southern extremity of Area 2 into Area 1 which was not evident in the forecasts from area centroids. Furthermore, the hindcasts suggested a potential for recruitment into Areas 1, 3, 4 and 5 from adjacent locations predicted to contain sponges that are outside any existing closures and in some cases from identified VMEs (Table 6).

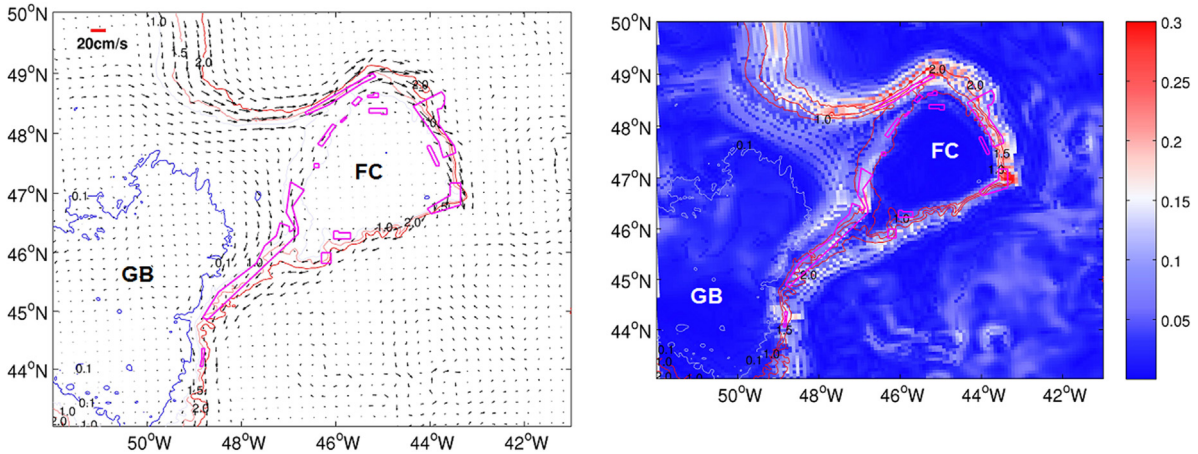

Fig. 5. Modelled on-bottom currents (left panel; scale bar upper left corner) and map of current speeds (m/s; right panel). Depth contours (km $\times 10^3$) and areas closed by NAFO to protect VMEs (purple outline) are shown. Every third vector was plotted to avoid crowding. GB = Grand Bank; FC = Flemish Cap.

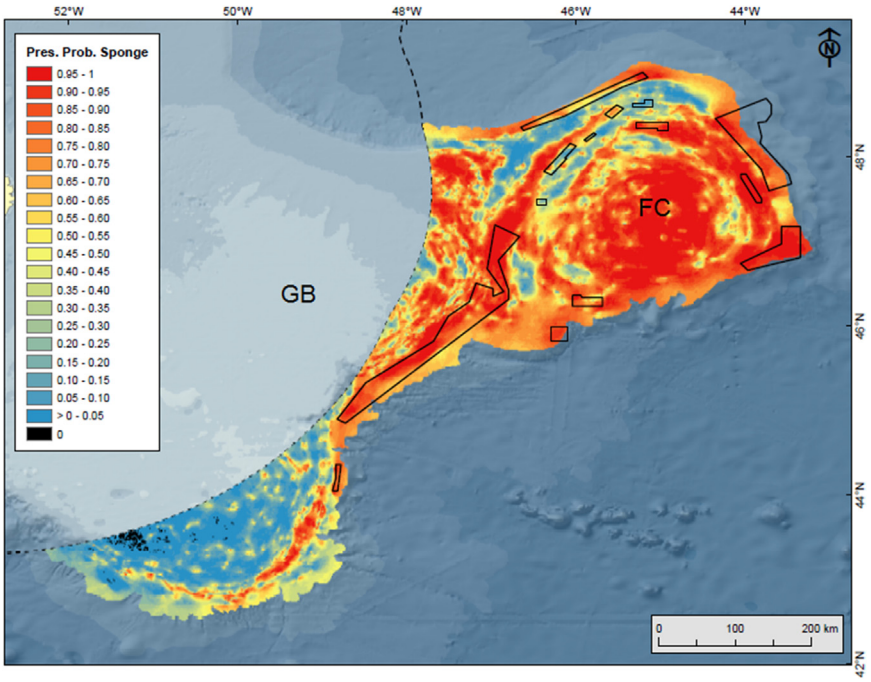

Fig. 6. Probability of sponge presence from an unbalanced random forest model. Prevalence was 56% and sponge presence is predicted above that threshold. The dashed line represents the boundary of Canadian jurisdiction. Areas closed to protect vulnerable marine ecosystems are outlined in black. GB = Grand Bank; FC = Flemish Cap.

3.3.2. *Areas closed to protect sea pens*

Hindcast passive-particle drifts, over 2-week durations at 100 m depth, leading to the centroids of areas closed to protect sea pens, other than Area 2, mostly originated in locations with a high probability of sea pen occurrence (Table 5, Fig. 10). For Areas 7–12 and 14, the average probability of sea pen occurrence at the point of origin was 81% and the minimum 10%. The average increased to 91% and 86% in summer and autumn respectively. In summer, the particles tracked in a clockwise direction around Flemish Cap, while in the autumn they tracked anti-clockwise. The points of origin of drifts to the centroid of Area 2 had much lower probabilities of sea pen occurrence.

Over drift durations of one month, the trajectories leading to the centroids originated mostly from areas with a lower probability of sea pen occurrence (average 61%: Table 5), though they were higher in the summer (average 80%). With drift durations of 3 months, only Areas 7 and 14 showed points of origin in areas of high probability of sea pen occurrence. Areas 7, 8, 9, 11, 12 and 14 may draw recruitment from nearby areas that have been identified as sea pen VMEs (NAFO, 2013), but not yet protected (Table 6, Fig. 10).

Most of the equivalent surface drifts originated outside the study area. However, drifts of 2 weeks duration, leading to the centroids of Area 11 (in spring) and Area 14 (in summer and autumn) originated from areas with 65%, 95% and 95% probability of sea pen occurrence, respectively.

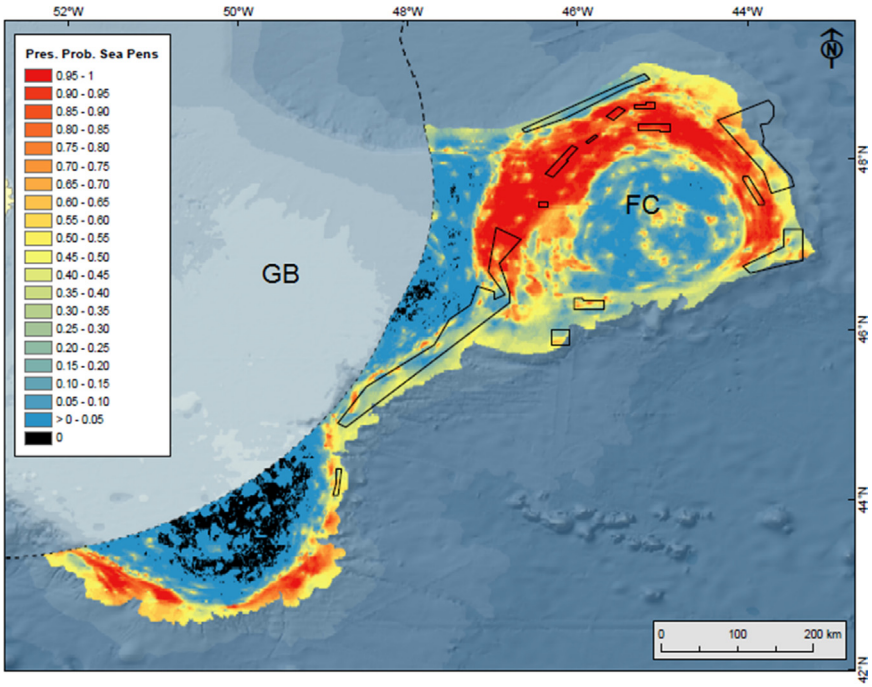

Fig. 7. Probability of sea pen presence from an unbalanced random forest model. Prevalence was 35% and presence of sea pens is predicted above that threshold. The dashed line represents the boundary of Canadian jurisdiction. Areas closed to protect vulnerable marine ecosystems are outlined in black. GB = Grand Bank; FC = Flemish Cap.

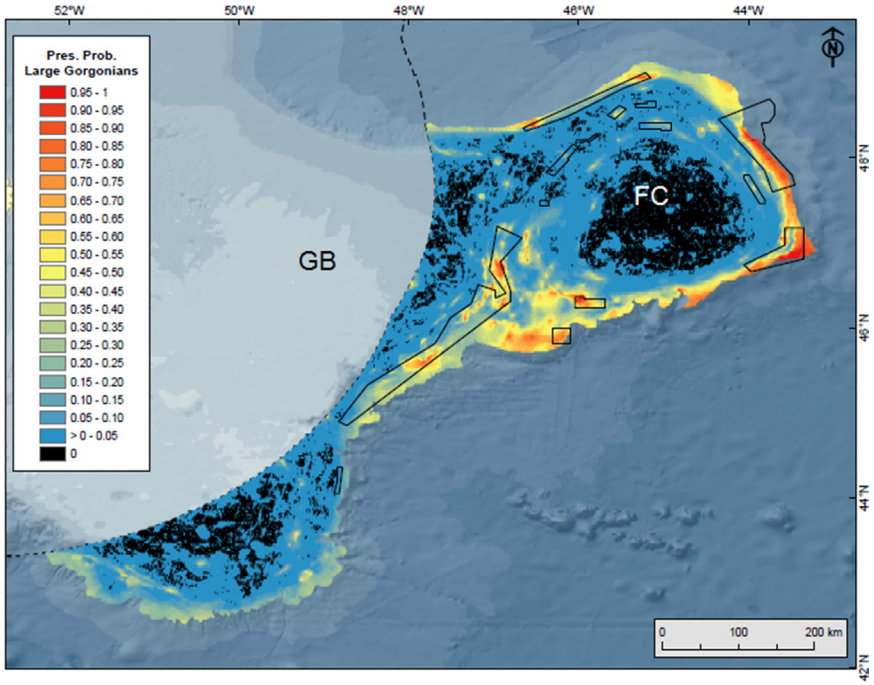

Fig. 8. Probability of large gorgonian coral presence from an unbalanced random forest model. Prevalence was 6% and presence of large gorgonian corals is predicted above that threshold. The dashed line represents the boundary of Canadian jurisdiction. Areas closed to protect vulnerable marine ecosystems are outlined in black. GB = Grand Bank; FC = Flemish Cap.

3.3.3. Areas closed to protect large gorgonian corals

Hindcast passive-particle drifts, at 100 m depth, to the centroids of areas closed to protect large gorgonian corals mostly originated in locations with a low probability of coral occurrence (Table 5). Only Area 13 had the potential to draw recruitment, regardless of drift duration, from areas where there was moderate to high probability of occurrence of these species (Table 5, Fig. 11). In the spring, the origin of the 2-week drift path to the centroid of that area was immediately outside its boundary (Table 6). Area 4 also had potential sources within its own boundaries or close by (Fig. 11). For Area 5, drifts with durations of 3 months in autumn led from sources with 71% probability of large gorgonian coral presence.

For surface drifts, 14 of the 48 hindcasts (by season and duration) had drift origins within the study area, although only 4 originated from areas with predicted large gorgonian presence. With PLD of 2 weeks in the autumn, Area 5 had sources with 35% probability of large gorgonian coral presence, while the equivalent hindcast for the spring showed an origin with 65% probability. For Area 13, drifts with durations of 2 weeks in summer and of 1 month in spring led from sources with 33% and 10% probability of large gorgonian coral presence.

3.4. Overlying oceanic water masses

Weak horizontal temperature and salinity gradients overlie the closed areas on the west and north slopes of Flemish Cap, while the eastern and southern slopes are under strong horizontal gradients, warming and becoming more saline towards the east and southeast respectively (Fig. 12). The closed areas on the Cap underlie slightly warmer, saltier near-surface (100 m depth) water than do those in Flemish Pass and on the Tail of Grand Bank.

At 1500 m, Areas 5 and 6 have large parts of their area influenced by cold (3.2 °C) water which is slightly saltier over Area 6 than over Area 5. The higher salinity may result from deeper water masses being elevated by topographic forcing in the relatively shallow Orphan Basin, northwest of Area 6.

4. Discussion

The 14 closed areas on Flemish Cap were put in place by NAFO to protect VMEs from destructive fishing practices in response to a series of UNGA sustainable fisheries resolutions (e.g., UNGA resolutions 57/141 (2002), 59/25 (2004), 61/105 (2006), 64/72 (2009), 66/68 (2011), 71/123 (2016): http://www.un.org/depts/los/general_assembly/general_assembly_resolutions.htm accessed on 23 May 2018). Although in September 2018 the NAFO Commission voted to reopen one of those areas (Area 14) to fishing in January 2019. The delineation of those closed areas (NAFO, 2017) simultaneously considered the locations of VMEs and fishing, however the long-term ability for the closed areas to reach their conservation goals requires further knowledge of connectivity between closed areas and identification of sources of recruitment to those areas that may not be under current protection.

We have shown that there are many knowledge gaps in the reproductive and larval biology of the dominant sponge and coral species in this region (and elsewhere), which prevents construction of biophysical models tailored to the biological traits of those conservation targets. Notwithstanding this constraint, the scope for effective connectivity of gametes and larvae can be evaluated using physical models as a first approximation of dispersal kernels (Young et al., 2012). Our results show that the seabed topography of the Flemish Cap region has such a strong influence on ocean circulation from 100 m to the sea floor, that the connectivity paths between closed areas, or lack thereof, reported here are likely to be typical. This is despite the limitations of only producing particle trajectories for the surface and 100 m depth and our subsequent extrapolation of those results based on NEMO circulation models for 1000 m and the sea floor.

4.1. Structural connectivity

For most area/season/drift-depth/duration combinations in our analyses, passive particles were modelled as being exported from the study area and entrained in the North Atlantic Current (NAC), especially for surface drifts and for longer drift durations (Fig. 2). The maximum velocity for the North Atlantic Current at the surface is 100 cm s^{-1} (Krauss et al., 1987) which explains this result. Current

Table 5
Probability of occurrence of conservation-target taxa from species distributions models at the points of origin of drift trajectories hindcast at 100 m depth and leading to centroids of closed areas. (–: predicted point of origin lies outside the spatial extent of the species distribution models; *: value below species prevalence and so taxon not predicted to occur at hindcast endpoint; LGC = large gorgonian coral).

Closed area	Taxon	Drift duration	Season Spring	Summer	Autumn	Winter
1	Sponge	2 weeks	0.81	0.83	0.82	0.69
2	Sponge	2 weeks	0.55*	0.63	0.91	0.94
3	Sponge	2 weeks	0.84	0.73	0.83	0.73
4	Sponge	2 weeks	1.00	0.94	–	0.98
5	Sponge	2 weeks	0.90	0.46*	0.85	0.94
6	Sponge	2 weeks	–	–	–	–
1	Sponge Ground	2 weeks	0.03*	0.82	0.01*	0.03*
2	Sponge Ground	2 weeks	0.00*	0.00*	0.00*	0.00*
3	Sponge Ground	2 weeks	0.27	0.02*	0.35	0.55
4	Sponge Ground	2 weeks	0.97	0.01*	0.65	0.87
5	Sponge Ground	2 weeks	0.02*	0.13	0.68	0.01*
6	Sponge Ground	2 weeks	0.45	0.41	–	0.48
2	Sea Pen	2 weeks	0.26*	0.06*	0.00*	0.00*
7	Sea Pen	2 weeks	0.66	0.95	0.61	0.64
8	Sea Pen	2 weeks	0.79	0.78	0.97	0.95
9	Sea Pen	2 weeks	0.13*	0.77	0.98	0.10*
10	Sea Pen	2 weeks	0.80	0.99	0.86	0.81
11	Sea Pen	2 weeks	1.00	1.00	0.97	0.97
12	Sea Pen	2 weeks	0.90	0.99	0.95	0.87
14	Sea Pen	2 weeks	0.96	0.91	0.67	0.76
2	Sea Pen	1 month	–	–	–	–
7	Sea Pen	1 month	0.65	0.95	0.11*	0.15*
8	Sea Pen	1 month	0.90	0.58	0.87	0.12*
9	Sea Pen	1 month	–	0.86	0.84	0.30*
10	Sea Pen	1 month	–	0.98	0.19*	0.33*
11	Sea Pen	1 month	0.33*	0.83	0.98	0.84
12	Sea Pen	1 month	–	0.98	0.85	0.34*
14	Sea Pen	1 month	0.93	0.98	0.32*	0.11*
2	Sea Pen	3 months	–	–	–	–
7	Sea Pen	3 months	0.95	0.97	0.50	0.97
8	Sea Pen	3 months	–	–	0.33*	–
9	Sea Pen	3 months	–	–	0.31*	–
10	Sea Pen	3 months	–	–	–	–
11	Sea Pen	3 months	–	–	0.50	–
12	Sea Pen	3 months	–	–	0.48	–
14	Sea Pen	3 months	0.02*	0.92	0.30*	0.04*
2	LGC	2 weeks	0.01*	0.00*	0.00*	0.00*
4	LGC	2 weeks	0.20	0.01*	–	0.30
5	LGC	2 weeks	0.03*	0.02*	0.28	0.17
13	LGC	2 weeks	0.71	0.46	0.35	0.40
2	LGC	1 month	–	–	–	–
4	LGC	1 month	0.29	0.00*	–	0.03*
5	LGC	1 month	0.01*	0.02*	0.06*	0.00*
13	LGC	1 month	0.41	0.21	–	0.61
2	LGC	3 months	–	–	–	–
4	LGC	3 months	0.09	0.00*	–	0.00*
5	LGC	3 months	0.03*	–	0.71	0.02*
13	LGC	3 months	0.01*	–	0.10	0.00*

speeds of 30 cm s^{-1} are common along the steep slopes even at 1000 m depth, but in contrast to the surface trajectories, strongly steer passive particles along depth contours. With drifts at 100 m depth, eight of the 14 closed areas showed potential for particle retention in, or return to, points within or near their boundaries (≤ 10 km distant) at certain seasons. The areas with endpoints within their boundaries were either large, and thus able to contain entire dispersal kernels (Areas 2, 4, 5), or else positioned within a weak gyre over a knoll (Areas 3 and 13). At 1000 m and at the sea floor, retention potential increases as the currents weaken.

Structural connectivity between closed areas was indicated in a number of instances (Table 7). Unidirectional connection at 100 m depth from the southern portion of Area 2, in Flemish Pass, to Area 1, is consistent with the flow of the Labrador Current (LC). However, the speed of the current and the large size of Area 2 (5421 km^2) combined to generally favour retention of modelled particles within that closed area. Over Flemish Cap, a Taylor column generated by the anti-cyclonic circulation has an isolating effect on the central portion of the Cap (Gil et al., 2004), enhancing the connectivity among areas there. Conversely, the small sizes of the sea pen closed areas (Table 1) decreased the likelihood of full connections. Thus, seven of the nine connecting trajectories ended outside of the boundaries of the recipient closed area (Table 3). Most of the connections between closed areas on Flemish Cap followed that anti-cyclonic circulation. However, cyclonic flows connected some of them in the autumn and in one case, summer. Area 9 emerged as key, not only connecting to the greatest number of other closed areas, but doing so in both cyclonic and anti-cyclonic directions. The surface flows in the Flemish Cap region are strongly influenced by the winds which are from the west-northwest in the early spring, from the southwest in late spring and summer, and are stronger in autumn and winter. The Labrador Current (Han, 2005), Gulf Stream (Fu et al., 1987) and NAC (Yaremchuk et al., 2001) all have clear seasonality, and seasonal variations in wind fields affecting those interacting currents likely led to the reverse flows shown by the tracking model. The effects of seasonality are expected to be reduced with depth below 100 m, however strong inter-annual variations have been reported in previous studies (e.g., Wang et al., 2016).

Because Webdrogue does not address random perturbations in water movements, their effects on structural connectivity are not reflected in our results. Introducing random walk simulations (Spivakovskaya et al., 2006) into the Webdrogue tracking model might help to incorporate small-scale temporal water movements that could be biologically relevant. Rare events could create other temporary connections, and might be important to very long-lived species, such as gorgonian corals. However those cannot be effectively modelled.

4.2. Functional connectivity potential

Advancing understanding from structural to functional connectivity requires that the results of passive-particle tracking models be interpreted in light of information on the spawning seasons, drift depths and larval durations of the principal species (Gallego et al., 2017), most of which have not been sufficiently studied (Table 2). Our species distribution models show that the placement of closures on Flemish Cap and in Flemish Pass capture much of the predicted distributions of the conservation targets and provide boundaries for identification of functional dispersal kernels.

4.2.1. Sponges

Based on the available knowledge of the biological traits of sponges (Section 2.2.1), we selected physical models with a PLD of 2 weeks, run under all four seasonal fields, as the focus for our evaluation of functional connectivity. Areas closed to protect sponges (Areas 1–6) favour retention at 100 m depth and this attribute is likely to be strengthened near the sea floor where some of the closures extend to 2754 m (Table 1). Multiple water masses overlie these deep areas with Labrador Sea Water underlain by Northeast Atlantic Deep Water and below that oxygen-rich Denmark Strait Overflow Water, promoting potential impediment to vertical movement of larvae.

While the closed areas are large and produce larvae that are likely retained within them, other sources for recruitment were identified through hindcasting. For 2-week drift durations, hindcasting from Area 6 identified potential source areas to the west, on the Nose of Grand Bank (Fig. 9). Similarly, Area 1 has a high probability of drawing recruits in summer from sponge grounds upstream. The recognized

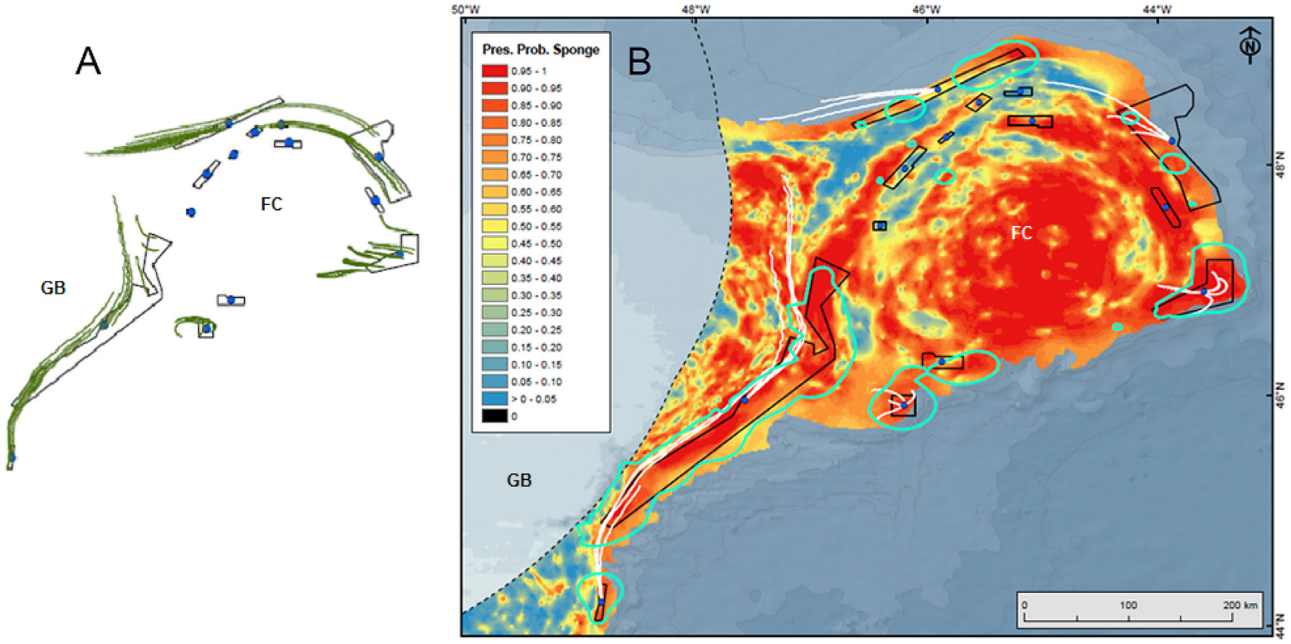

Fig. 9. Drift trajectories at 100 m depth hindcast over two week durations from each of closed Areas 1–6, which were closed to protect sponge grounds, A) Summer trajectories from 50 randomly placed start positions, and B) Trajectories from centroid start positions in each of four seasons (not colour coded), overlain on the probability of presence of sponges. Closed areas are indicated in black outline. Sponge VME polygons recognized by NAFO (2016) are indicted in light blue on the right panel. GB = Grand Bank; FC = Flemish Cap.

Table 6
Closed areas which may draw recruitment from adjacent areas open to fishing that are portions of the polygons recognized as vulnerable marine ecosystems (NAFO, 2013, 2016). Details of specific depths, seasons and drift durations are provided. (Sp = Spring; Su = Summer; A = Autumn; W = Winter; LGC = large gorgonian coral).

VME polygon	Drift depth	Closed area	Season	Drift duration(s)
Sponge	Surface	Area 3	Su	2 weeks
Sponge	Surface	Area 5	Sp	2 weeks
Sponge	100 m	Area 1	Sp, W	2 weeks
Sponge	100 m	Area 3	Sp, A, W	2 weeks
Sponge	100 m	Area 4	Su	2 weeks
Sea Pen	100 m	Area 7	Sp, W	3 months
Sea Pen	100 m	Area 8	Sp, A	2 weeks
Sea Pen	100 m	Area 8	A	1 month
Sea Pen	100 m	Area 9	A	1 month
Sea Pen	100 m	Area 11	Sp, A	2 weeks
Sea Pen	100 m	Area 11	A	1 month
Sea Pen	100 m	Area 12	Su, W	2 weeks
Sea Pen	100 m	Area 14	Sp	2 weeks
Sea Pen	100 m	Area 14	Su	1 month
Sea Pen	100 m	Area 14	Su	3 months
LGC	100 m	Area 13	Sp	2 weeks

sponge VMEs (NAFO, 2013, 2016) are not fully protected within the existing closed areas and our analyses have shown that Area 3 and Area 4 may rely on recruitment from unprotected VME outside the closure boundaries (Table 6, Fig. 9).

4.2.2. Sea pens

The closed areas (Areas 2, 7–12, 14) to protect sea pens show physical connectivity and appear to form a weak network over Flemish Cap, primarily operating at 100 m. Scenarios with PLD for all three time periods produced connections between closed areas. Although PLD and larval position in the water column is unknown for this group (Section 2.2.1), the depth range of these areas on Flemish Cap is 578–1177 m (Table 1). At such depths larvae would be exposed to multiple cores of LSW (Yashayaev, 2007; Yashayaev and Loder, 2016) before reaching the surface. Should they succeed in migrating to surface waters they would be advected by the NAC away from the Cap over deep water to 4000 m or more.

Spawning season has been identified for the dominant taxa. For *Anthoptilum grandiflorum* and *Halipteris finmarchica*, spawning in spring/early summer, there is potential for dispersal at 100 m depth from Area 12 to Area 7 and from Area 9 to Area 14. For summer spawning of those species and *Pennatula aculeata*, four connections were identified. For the winter spawning *Funiculina quadrangularis*, there is potential for connectivity from Area 9 to Area 8, and perhaps between Areas 12, 7 and 8 when buffers around the closed areas are considered (Tables 3, 7).

The areas on Flemish Cap that were closed to protect sea pens are small relative to the regional distribution of those species (Fig. 7; Murillo et al., 2010) and much of the area recognized as VME has been left open to fishing (NAFO, 2016). Hindcast modelling indicated that six of these eight areas may draw on source populations identified as VMEs but still open to potential fishing (Table 6, Fig. 10). Area 11 is of special concern as it is small (Table 1), shows limited retention potential and is not likely connected with other areas, instead relying on areas to the west and north-northwest for recruitment depending upon the season (Fig. 10). The probability of source populations arising from the VME areas adjacent to the closures is highest for PLD of 2 weeks and 1 month and becomes unlikely for PLD of 3 months except for Area 7. Area 14 draws on recruitment from the area to its north north-west with PLD of 2 weeks in summer (Fig. 10). This area falls between Area 14 to the south and Area 8 to the northwest and has been discussed by NAFO (2016) as an area for potential closure.

4.2.3. Large gorgonian corals

As for the sea pens, there is little information on the key biological traits required to parameterize the physical model, except for spawning season in some (Section 2.2.2). However, all areas closed to protect large gorgonian corals (Areas 2, 4, 5, 13) showed passive-particle retention at 100 m depth in some seasons, particularly Spring with short PLD (Tables 4, 7). The similarity of currents at greater depths suggests that there would also be retention at deeper larval drift depths as proposed for sponges in these same areas (Section 4.2.1). Moreover,

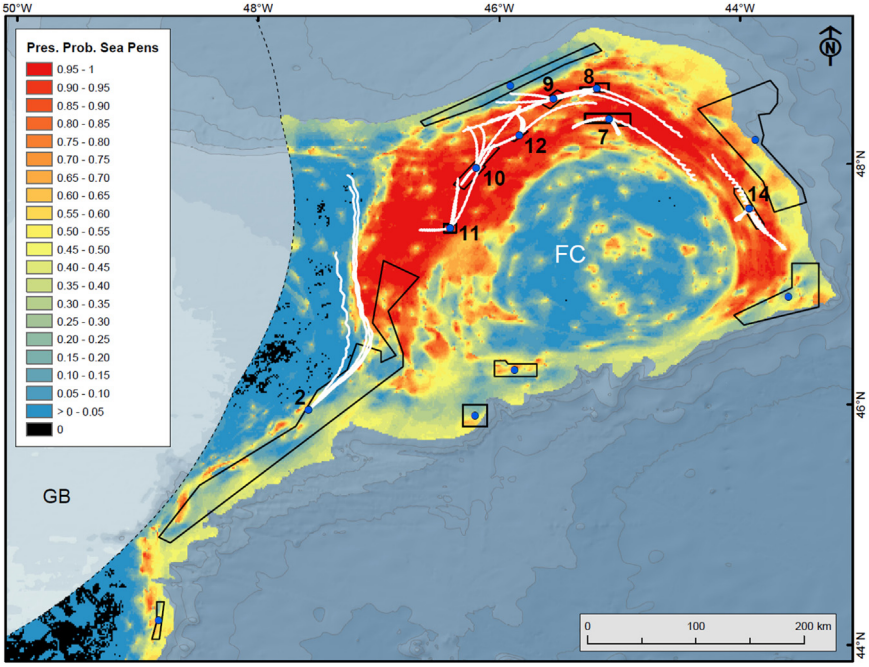

Fig. 10. Drift trajectories at 100 m depth hindcast over two week durations starting within each of the Areas closed to protect sea pens (Table 1). Models shown were run for four seasons (not colour coded) from a centroid start position, overlain on the probability of presence of sea pens. GB = Grand Bank; FC = Flemish Cap.

hindcast trajectories showed that Area 13 has potential sources of recruitment from areas with high probability of coral presence to the southeast of the closure, both inside the recognized VME polygon and beyond (Fig. 10).

4.3. Management implications

The incremental establishment of the closed areas meant that there was no collective "design" to their placement; however, they could qualify after the fact as a "network" of protected areas. Such areas should include the following design criteria: representativeness, replication, viability, precautionary design, permanence, maximum connectivity, resilience, size and shape (WCPA/IUCN, 2007). This collection of closed areas is representative of the VME habitats, and is replicated for sponges, sea pens and large gorgonian corals. However small gorgonian corals are only protected in one area and so do not have replication built into their protection at this time (Table 1).

Viability, connectivity, resilience and size/shape are linked properties which are all addressed to a certain degree in our study. However, our results describe structural connectivity among the closed areas and while we hypothesize functional linkages in light of the scant biological information we have on the key species, we cannot confirm effective connectivity. Nevertheless, we have provided realistic hypotheses for management under a precautionary approach which is included as an aspect of the network design criteria (WCPA/IUCN, 2007).

For sponges, the large areas that have been protected are likely to be

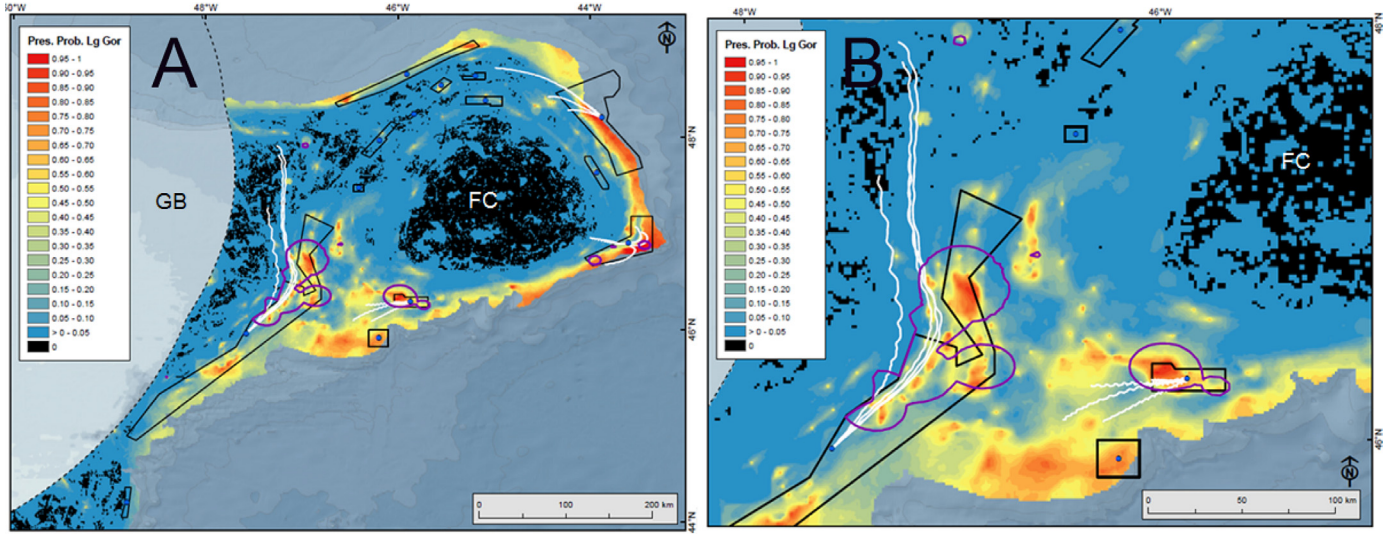

Fig. 11. Drift trajectories at 100 m depth hindcast over two week durations A) starting within each of Areas 2, 4, 5 and 13, which were closed to protect large gorgonian corals; B) close-up of the southern Flemish Pass (Area 2) and Beothuk Knoll (Area 13). Models were run for four seasons (not colour coded) from a centroid start position, overlain on the probability of presence of large gorgonian corals. Large gorgonian coral VME polygons recognized by NAFO (2016) are indicted in purple. GB = Grand Bank; FC = Flemish Cap.

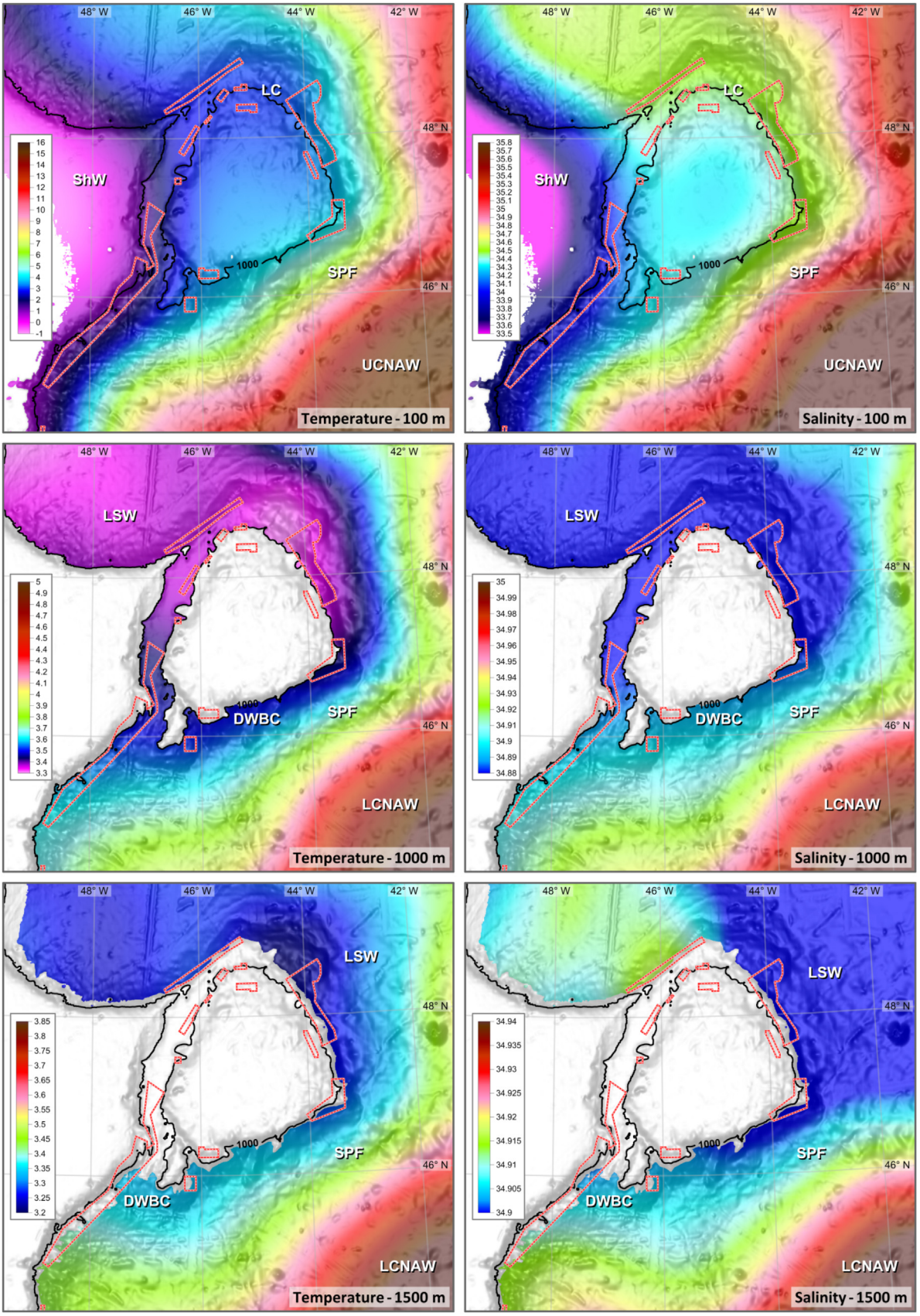

Fig. 12. Horizontal water property maps for temperature (left) and salinity (right) and currents at 100 m, 1000 m, and 1500 m depths (top to bottom). LSW = Labrador Sea Water; ShW = Shelf Water; SPF = Subpolar Front; UCNAW = Upper Central North Atlantic Water; DWBC = Deep Western Boundary Current; LCNAW = Lower Central North Atlantic Water; GB = Grand Bank; FC = Flemish Cap. Closed Areas are indicated in pink. Note that the colour scales differ between maps in order to differentiate water masses at depth.

Table 7
Summary of structural connectivity and retention for each of the closed areas linking areas with the same conservation targets. Bracketed connections end within 10 km of the named closed areas. *: connection revealed through hindcasting from random start points.

Closed area	Connectivity with drift depth of 100 m	Retention with drift depth of 100 m
Area 1	–	–
Area 2	Area 1*	Yes
Area 3	–	Yes
Area 4	–	Yes
Area 5	–	Yes
Area 6	–	–
Area 7	(Area 8)	–
Area 8	(Area 14)	–
Area 9	Area 8 (Area 10, Area 14)	(Yes)
Area 10	(Area 14)	–
Area 11	–	(Yes)
Area 12	Area 7, (Area 10)	–
Area 13	–	Yes
Area 14	(Area 9)	(Yes)

self-recruiting, and hence viable (WCPA/IUCN, 2007) but Areas 1, 3, 4 and 5 should be increased to include more of their VME areas which are additional sources of recruitment (Table 6). Area 6 appears to be the most isolated and likely draws recruitment to its western portion from unprotected areas at similar depths on the Nose of Grand Bank. Extension of the Area 6 closure to the west should be evaluated.

The identification of a sea pen network, connecting some of the closed areas on Flemish Cap, has implications for the longer term protection of those areas, particularly Area 9 which protects a potential source population for up to three other areas in the network. However, many of the areas are not sufficiently large to meet the criteria of viability and size, with impacts from nearby fishing potentially affecting population demographics (WCPA/IUCN, 2007). Area 9 is relatively small and consideration could be given to its expansion to ensure that its connectivity potential is protected. Area 11 which showed neither strong connections nor retention appears to rely on recruitment from fished sea beds and therefore is more vulnerable than other closed areas. Area 14, the last of the sea pen closures to be put in place, draws on recruitment from unprotected VME (NAFO, 2016) to the north north-west (Fig. 10) and that area should be reconsidered for protection to strengthen the connectivity of the sea pen network with this new evidence for its value in the sea pen network. The recent decision to reopen Area 14 to fishing compromises this network. Further, it calls into question the permanency of these management actions, which is an element of network design.

Large gorgonian corals, like sponges, appear to be viable through particle retention in the large closed areas. The smaller Area 13 has potential sources of recruitment from areas outside of the closure, both inside the recognized VME polygon and beyond. Indeed, across all of the closed areas, eleven may rely on recruitment from areas open to fishing (NAFO, 2013) (Table 6) and encompassing more of the recognized VME within the closures would have conservation benefits.

Acknowledgements

We thank T. Kenchington, A. Drozdowski and L. Beazley at the Bedford Institute of Oceanography, and two anonymous reviewers, for their very helpful suggestions for improvement of earlier drafts of this paper. We also thank our colleagues in the NAFO Working Group on Ecosystem Science Assessment (WGESA) for their helpful comments and suggestions.

Funding

This work was supported by Fisheries and Oceans, Canada's International Governance Strategy, awarded to EK; this work is a Canadian and Spanish CSIC contribution to the SponGES project - part of the European Union's Horizon 2020 research and innovation programme under grant agreement no. 679849. The EU groundfish surveys in the NAFO area were co-funded by the Spanish Institute of Oceanography (IEO), the Portuguese Institute for Sea and Atmosphere (IPMA), the Spanish Institute for Marine Research Superior Council of Scientific Investigations (IIM-CSIC) and the European Union through the European Maritime and Fisheries Fund (EMFF) within the National Program of collection, management and use of data in the fisheries sector and support for scientific advice regarding the Common Fisheries Policy.

References

Andrello, M., Guilhaumon, F., Albouy, A., Parravicini, V., Scholtens, J., Verley, P., Barange, M., et al., 2017. Global mismatch between fishing dependency and larval supply from marine reserves. Nat. Commun. 8, 16039.
Alabia, I.D., Saitoh, S.-I., Igarashi, H., Ishikawa, Y., Usui, N., Kamachi, M., Awaji, T., et al., 2016. Ensemble squid habitat model using three-dimensional ocean data. ICES J. Mar. Sci. 73, 1863–1874.
Baguette, M., Blanchet, S., Legrand, D., Stevens, V.M., Turlure, C., 2013. Individual dispersal, landscape connectivity and ecological networks. Biol. Rev. Camb. Philos. Soc. 88, 310–326.
Baillon, S., Hamel, J.-F., Mercier, A., 2015. Protracted oogenesis and annual reproductive periodicity in the deep-sea pennatulacean *Halipteris finmarchica* (Anthozoa, Octocorallia). Mar. Ecol. 36, 1364–1378.
Baillon, S., Hamel, J.-F., Wareham, V.E., Mercier, A., 2014. Seasonality in reproduction of the deep-water pennatulacean coral *Anthoptilum grandiflorum*. Mar. Biol. 161, 29–43.
Bautista-Guerrero, E., Carballo, J.L., Maldonado, M., 2010. Reproductive cycle of the coral-excavating sponge *Thoosa mismalolli* (Clionaidae) from Mexican Pacific coral reefs. Invert. Biol. 129, 285–296.
Beazley, L., Kenchington, E., Yashayaev, I., Murillo, F.J., 2015. Drivers of epibenthic megafaunal composition in the sponge grounds of the Sackville Spur, northwest Atlantic. Deep Sea Res. Part I Oceanogr. Res. Pap. 98, 102–114.
Ben-David-Zaslow, R., Benayahu, Y., 1996. Longevity, competence and energetic content in planulae of the soft coral *Heteroxenia fuscescens*. J. Exp. Mar. Biol. Ecol. 206, 55–68.
Ben-David-Zaslow, R., Benayahu, Y., 1998. Competence and longevity in planulae of several species of soft corals. Mar. Ecol. Prog. Ser. 163, 235–243.
Borchiellini, C., Chombard, C., Manuel, M., Alivon, E., Vacelet, J., Boury-Esnault, N., 2004. Molecular phylogeny of Demospongiae: implications for classification and scenarios of character evolution. Mol. Phylogenet. Evol. 32, 823–837.
Breiman, L., 2001. Random forests. J. Mach. Learn. Res. 45, 5–32.
Brock, R.J., Kenchington, E., Martinez-Arroyo, A., 2012. Scientific Guidelines for Designing Resilient Marine Protected Area Networks in a Changing Climate. Commission for Environmental Cooperation, Montreal, Canada (95pp).
Cárdenas, P., Rapp, H.T., Klitgaard, A.B., Best, M., Thollesson, M., Tendal, O.S., 2013. Taxonomy, biogeography and DNA barcodes of *Geodia* species (Porifera, Demospongiae, Tetractinellida) in the Atlantic boreo-arctic region. Zool. J. Linn. Soc. 169, 251–311.
Chia, F.S., Crawford, B.J., 1973. Some observations on gametogenesis, larval development and substratum selection of the sea pen *Ptilosarcus guerneyi*. Mar. Biol. 23, 73–82.
Coma, R., Ribes, M., Zabala, M., Gili, J.-M., 1995. Reproduction and cycle of gonadal development in the Mediterranean gorgonian *Paramuricea clavata*. Mar. Ecol. Prog. Ser. 117, 173–183.
Cowen, R.K., Sponaugle, S., 2009. Larval dispersal and marine population connectivity. Annu. Rev. Mar. Sci. 1, 443–466.
Crooks, K.R., Sanjayan, M., 2006. Connectivity Conservation. Cambridge University Press, Cambridge.
Dahan, M., Benayahu, Y., 1998. Embryogenesis, planulae longevity, and competence in the octocoral *Dendronephthya hemprichi*. Invertebr. Biol. 117, 271–280.
Eckelbarger, K.J., Tyler, P.A., Langton, R.W., 1998. Gonadal morphology and gametogenesis in the sea pen *Pennatula aculeata* (Anthozoa: pennatulacea) from the Gulf of Maine. Mar. Biol. 132, 677–690.
Edwards, D.C.B., Moore, C.G., 2008. Reproduction in the sea pen *Pennatula phosphorea* (Anthozoa: pennatulacea) from the west coast of Scotland. Mar. Biol. 155, 303–314.
Edwards, D.C.B., Moore, C.G., 2009. Reproduction in the sea pen *Funiculina quadrangularis* (Anthozoa: pennatulacea) from the west coast of Scotland. Estuar. Coast. Shelf Sci. 82, 161–168.
Fredj, E., Carlson, D.F., Amitai, Y., Gozolchiani, A., Gildor, H., 2016. The particle tracking and analysis toolbox (PaTATO) for Matlab. Limnol. Oceanogr. Methods 14, 586–599.
Fu, L., Vazquez, J., Parke, M.E., 1987. Seasonal variability of the Gulf Stream from satellite altimetry. J. Geophys. Res. 92, 749–754.
Gallego, A., Gibb, F.M., Tullet, D., Wright, P.J., 2017. Bio-physical connectivity patterns of benthic marine species used in the designation of Scottish nature conservation marine protected areas. ICES J. Mar. Sci. 74, 1797–1811.
Garrone, R., 1974. Ultrastructure d'une "gemmule armée" planctonique d'éponge Clionidae. inclusions fibrillaires etgenèse du collagène. Arch. Anat. Microsc. Morphol. Exp. 63, 163–182.

Gil, J., Sánchez, R., Cerviño, S., Garabana, D., 2004. Geostrophic circulation and heat flux across the Flemish Cap, 1988–2000. J. Northw. Atl. Fish. Sci. 34, 63–83.
Grant, A., 1983. On the evolution of brood protection in marine benthic invertebrates. Am. Nat. 122 (549-444).
Guijarro, J., Beazley, L., Lirette, C., Kenchington, E., Wareham, V., Gilkinson, K., Koen-Alonso, M., et al., 2016a. Species distribution modelling of corals and sponges from research vessel survey data in the Newfoundland and Labrador Region for use in the dentification of significant benthic areas. Can. Tech. Rep. Fish. Aquat. Sci. 3171 (vi + 126p).
Guijarro, J., Beazley, L., Lirette, C., Wang, Z., Kenchington, E., 2016b. Characteristics of environmental data layers for use in species distribution modelling in the Newfoundland and Labrador Region. Can. Tech. Rep. Fish. Aquat. Sci. 3187 (viii + 325p).
Hadfield, M.G., Strathmann, M.F., 1996. Variability, flexibility and plasticity in life histories of marine invertebrates. Oceanol. Acta 19, 323–334.
Han, G., 2005. Wind-driven barotropic circulation off Newfoundland and Labrador. Cont. Shelf Res. 25, 2084–2106.
Han, G., Lu, Z., Wang, Z., Helbig, J., Chen, N., de Young, B., 2008. Seasonal variability of the Labrador Current and shelf circulation off Newfoundland. J. Geophys. Res. 113, C10013. https://doi.org/10.1029/2007JC004376.
Hannah, C.G., Shore, J.A., Loder, J.W., 2000. The retention-drift dichotomy on Browns Bank: a model study of interannual variability. Can. J. Fish. Aquat. Sci. 57, 2506–2518.
Hanski, I., 1998. Metapopulation dynamics. Nature 396, 41–49.
Kahng, S.E., Benayahu, Y., Lasker, H.R., 2011. Sexual reproduction in octocorals. Mar. Ecol. Prog. Ser. 443, 265–283.
Kenchington, E., Murillo, F.J., Lirette, C., Sacau, M., Koen-Alonso, M., Kenny, A., Ollerhead, N., et al., 2014. Kernel density surface modelling as a means to identify significant concentrations of vulnerable marine ecosystem indicators. PLoS One 9 (10), e109365.
Knudby, A., Lirette, C., Kenchington, E., Murilo, F.J., 2013a. Species distribution models of black corals, large gorgonian corals and sea pens in the NAFO Regulatory Area. N6276. NAFO SCR Doc. 13/78, p. 17.
Knudby, A., Kenchington, E., Murillo, F.J., 2013b. Modeling the distribution of *Geodia* sponges and sponge grounds in the northwest Atlantic Ocean. PLoS One 8, e82306.
Krauss, W., Fahrbach, E., Aitsam, A., Elken, J., Koske, P., 1987. The North Atlantic Current and its associated eddy field southeast of Flemish Cap. Deep-Sea Res. 34, 1163–1185.
Lacharité, M., Metaxas, A., 2013. Early life history of deep-water gorgonian corals may limit their abundance. PLoS One 8 (6), e65394. https://doi.org/10.1371/journal.pone.0065394.
Liaw, A., Wiener, M., 2002. Classification and regression by random forest. R. News 2, 18–22.
Lundberg, J., Moberg, F., 2003. Mobile link organisms and ecosystem functioning: implications for ecosystem resilience and management. Ecosystems 6, 87–98.
Maldonado, M., 2004. Choanoflagellates, choanocytes, and animal multicellularity. Invert. Biol. 123, 1–22.
Maldonado, M., 2006. The ecology of the sponge larva. Can. J. Zool. 84, 175–194.
Maldonado, M., Aguilar, R., Bannister, R.J., Bell, J.J., Conway, K.W., Dayton, P.K., Diaz, C., Gutt, J., Kelly, M., Kenchington, E.L.R., Leys, S.P., Pomponi, S.A., Rapp, H.T., Rutzler, K., Tendal, O.S., Vacelet, J., Young, C.M., 2017. Sponge grounds as key marine habitats: a synthetic review of types, structure, functional roles, and conservation concerns. In: Rossi, S., Bramanti, L., Gori, A., Orejas, C. (Eds.), Marine Animal Forests: The Ecology of Benthic Biodiversity Hotspots Marine Animal Forests. Springer International Publishing, Switzerland, pp. 1–39.
Maldonado, M., Bergquist, P.R., 2002. Phylum Porifera. In: Young, C.M., Sewell, M.A., Rice, M.E. (Eds.), Atlas of Marine Invertebrate Larvae. Academic Press, San Diego, pp. 21–50.
Maldonado, M., Riesgo, A., 2008. Reproduction in the phylum Porifera: a synoptic overview. Treb. Soc. Cat. Biol. 59, 29–49.
Maldonado, M., Young, C.M., 1996. Effects of physical factors on larval behavior, settlement and recruitment of four tropical demosponges. Mar. Ecol. Prog. Ser. 138, 169–180.
Mariani, S., Uriz, M.-J., Turon, X., 2005. The dynamics of sponge larvae assemblages from northwestern Mediterranean nearshore bottoms. J. Plankton Res. 27, 249–262.
Mariani, S., Uriz, M.-J., Turon, X., Alcoverro, T., 2006. Dispersal strategies in sponge larvae: integrating the life history of larvae and the hydrologic component. Oecologia 149, 174–184. https://doi.org/10.1007/s00442-006-0429-9.
Mercier, A., Hamel, J.-F., 2011. Contrasting reproductive strategies in three deep-sea octocorals from eastern Canada: *Primnoa resedaeformis*, *Keratoisis ornata*, and *Anthomastus grandiflorus*. Coral Reefs 30, 337–350.
Murillo, F.J., Durán Muñoz, P., Altuna, A., Serrano, A., 2011. Distribution of deep-water corals of the Flemish Cap, Flemish Pass, and the Grand Banks of Newfoundland (Northwest Atlantic Ocean): interaction with fishing activities. ICES J. Mar. Sci. 68, 319–332.
Murillo, F.J., Durán Muñoz, P., Cristobo, F.J., Rios, P., Gonzalez, C., Kenchington, E., Serrano, A., 2012. Deep-sea sponge grounds of the Flemish Cap, Flemish Pass and the Grand Banks of Newfoundland (Northwest Atlantic Ocean): distribution and species composition. Mar. Biol. Res. 8, 842–854.
Murillo, F.J., Kenchington, E., Gonzalez, C., Sacau, M., 2010. The use of density analyses to delineate significant concentrations of Pennatulaceans from trawl survey data. NAFO SCR Doc. 10/07 (Serial No. N5753, 7 pp).
Murillo, F.J., Serrano, A., Kenchington, E., Mora, J., 2016. Epibenthic assemblages of the Tail of the Grand Bank and Flemish Cap (northwest Atlantic) in relation to environmental parameters and trawling intensity. Deep Sea Res. Part I Oceanogr. Res. Pap. 109, 99–122.
NAFO, 2013. Report Proceedings of the 6th Meeting of the NAFO Scientific Council Working Group on Ecosystem Science and Assessment (WGESA). NAFO SCS Doc. 13/024, Serial No. N6277, p. 207.
NAFO, 2016. Report of the Scientific Council Meeting. NAFO SCS Doc. 16-14 Rev., Serial No. N6587, p. 296.
NAFO, 2017. Conservation and Enforcement Measures. NAFO/FC Doc. 17/01, Serial No. N6638, p. 188.
Pearse, J.S., 1994. Cold-water echinoderms break "Thorson's rule". In: Young, C.M., Eckelbarger, K.J. (Eds.), Reproduction, Larval Biology, and Recruitment in the Deep-Sea Benthos. Columbia Univ. Press, New York, pp. 26–43.
Phillips, S.J., Elith, J., 2013. On estimating probability of presence from use-availability or presence-background data. Ecology 94, 1409–1419.
Pineda, J., Hare, J.A., Sponaugle, S., 2007. Larval transport and dispersal in the coastal ocean and consequences for population connectivity. Oceanography 20, 22–39.
Piper, D.J.W., Campbell, D.C., 2005. Quaternary geology of Flemish Pass and its application to geohazard evaluation for hydrocarbon development. GAC Spec. Pap. 43, 29–43.
Pires, D.O., Castro, C.B., Silva, J.C., 2009. Reproductive biology of the deep-sea pennatulacean *Anthoptilum murrayi* (Cnidaria, Octocorallia). Mar. Ecol. Prog. Ser. 397, 103–112.
R Core Team, 2018. R: A Language and Environment for Statistical Computing. R Foundation for Statistical Computing, Vienna, Austria.
Radice, V.Z., Quattrini, A.M., Wareham, V.E., Edinger, E.N., Cordes, E.E., 2016. Vertical water mass structure in the North Atlantic influences the bathymetric distribution of species in the deep-sea coral genus *Paramuricea*. Deep Sea Res. Part I Oceanogr. Res. Pap. 116, 253–263.
Roberts, L.J., Maurer, B.A., Donovan, M., 2011. Choices and strategies for using a resource inventory database to support local wildlife habitat monitoring. In: Drew, C.A., Wiersma, Y.F., Huettmann, F. (Eds.), Predictive Species and Habitat Modeling in Landscape Ecology: Concepts and Applications. by Springer, New York, pp. 251–270.
Schneider, L., Kieke, D., Jochumsen, K., Colbourne, E., Yashayaev, I., Steinfeldt, R., Varotsou, E., et al., 2015. Variability of Labrador Sea Water exported through Flemish Pass during 1993–2013. J. Geophys. Res. 120, 5514–5533.
Shanks, A.L., 2009. Pelagic larval duration and dispersal distance revisited. Biol. Bull. 216, 373–385.
Shanks, A.L., Grantham, B.A., Carr, M.H., 2003. Propagule dispersal distance and the size and spacing of marine reserves. Ecol. Appl. 13, S159–S169.
Soong, K., 2005. Reproduction and colony integration of the sea pen *Virgularia juncea*. Mar. Biol. 146, 1103–1109.
Spetland, F., Rapp, H.T., Hoffmann, F., Tendal, O.S., 2007. Sexual reproduction of *Geodia barretti* Bowerbank, 1858 (Porifera, Astrophorida) in two Scandinavian fjords. In: Custódio, M.R., Hajdu, E., Lóbo-Hajdu, G., Muricy, G., Porifera Research: Biodiversity, Innovation and Sustainability Proceedings of the 7th International Sponge Symposium, Série Livros 28, Museu Nacional, Rio de Janeiro, Brazil, pp. 613–620.
Spivakovskaya, C., Deleersnijder, E., Heemink, A.W., 2006. Random walk model in case of iso- and diapycnal diffusion. In: Wesseling, P., Onate, E., Périaux, J. European Conference on Computational Fluid Dynamics ECCOMAS CFD, TU Delft, The Netherlands, 2006, pp. 1–19.
Tischendorf, L., Fahrig, L., 2000. On the usage and measurement of landscape connectivity. Oikos 90, 7–19.
Trégouboff, G., 1939. Sur les larves planctoniques d'éponges. C.R. Acad. Sci. Paris 208, 1245–1256.
Trégouboff, G., 1942. Contribution à la connaissance des larves planctonique d'éponges. Arch. Zool. Exp. Gen. 82, 357–399.
Tyler, P.A., Bronsdon, S.K., Young, C.M., Rice, A.L., 1995. Ecology and gametogenic biology of the genus *Umbellula* (Pennatulacea) in the North Atlantic Ocean. Int. Rev. Gesamt. Hydrobiol. 80, 187–199.
Vacelet, J., 1999. Planktonic armoured propagules of the excavating sponge *Alectona* (Porifera: demospongiae) are larvae: evidence from *Alectona wallichii* and *A. mesatlantica* sp. nov. Mem. Queensl. Mus. 44, 627–642.
Van Soest, R.W.M., Boury-Esnault, N., Vacelet, J., Dohrmann, M., Erpenbeck, D., De Voogd, N.J., Santodomingo, N., et al., 2012. Global diversity of sponges (Porifera). PLoS One 7 (4), e35105. https://doi.org/10.1371/journal.pone.0035105.
Waller, R.G., Stone, R.P., Johnstone, J., Mondragon, J., 2014. Sexual reproduction and seasonality of the Alaskan red tree coral, *Primnoa pacifica*. PLoS One 9 (4), e90893. https://doi.org/10.1371/journal.pone.0090893.
Wang, Z., Brickman, D., Greenan, B.J.W., Yashayaev, I., 2016. An abrupt shift in the Labrador Current system in relation to winter NAO events. J. Geophys. Res. Oceans 121, 5338–5349.
Watanabe, Y., 1978. The development of two species of *Tetilla* (demosponge). Nat. Sci. Rep. Ochanomizu Univ. 29, 71–106.
WCPA/IUCN, 2007. Establishing networks of marine protected areas: A guide for developing national and regional capacity for building MPA networks. Non-technical summary report, p. 16. ⟨https://www.cbd.int/doc/pa/tools/Establishing%20Marine%20Protected%20Area%20Networks.pdf⟩ (Accessed on 23 May 2018).
White, J.W., Schroeger, J., Drake, P.T., Edwards, C.A., 2014. The value of larval connectivity information in the static optimization of marine reserve design. Conserv. Lett. 7, 533–544.
Witte, U., 1996. Seasonal reproduction in deep-sea sponges — triggered by vertical particle flux? Mar. Biol. 124, 571–581.
Woollacott, R.M., 1990. Structure and swimming behavior of the larva of *Halichondria melanadocia* (Porifera: demospongiae). J. Morph. 205, 135–145.
Yaremchuk, M.I., Nechaev, D.A., Thompson, K.R., 2001. Seasonal variation of the North Atlantic Current. J. Geophys. Res. 106 (C4), 6835–6851.
Yashayaev, I., 2000. 12-Year Hydrographic Survey of the Newfoundland Basin: Seasonal

Cycle and Interannual Variability of Water Masses. ICES CM 2000/L:17 North Atlantic Processes, p. 17.
Yashayaev, I., 2007. Hydrographic changes in the Labrador Sea, 1960–2005. Prog. Oceanogr. 73, 242–276.
Yashayaev, I., Loder, J.W., 2016. Recurrent replenishment of Labrador Sea Water and associated decadal-scale variability. J. Geophys. Res. Oceans 121, 8095–8114.
Yashayaev, I., Seidov, D., 2015. The role of the Atlantic Water in multidecadal ocean variability in the Nordic and Barents Seas. Prog. Oceanogr. 132, 68–127.
Young, C.M., 1995. Behavior and locomotion during the dispersal phase of larval life. In: McEdward, L. (Ed.), Ecology of Marine Invertebrate Larvae. CRC Press, Florida, pp. 249–277.
Young, C.M., Devin, M., Jaeckle, W.B., Ekaratne, S., 1996a. The potential for ontogenetic vertical migration in larvae of deep-sea echinoids. Oceanol. Acta 19, 263–271.
Young, C.M., He, R., Emlet, R.B., Li, Y., Qian, H., Arellano, S.M., Van Gaest, A., Bennett, K.C., Wolf, M., Smart, T.I., Rice, M.E., 2012. Dispersal of deep-sea larvae from the intra-American Seas: simulations of trajectories using ocean models. Integr. Comp. Biol. 52, 483–496.
Young, C.M., Tyler, P.A., Gage, J.D., 1996b. Vertical distribution correlates with pressure tolerances of early embryos in the deep-sea asteroid *Plutonaster bifrons*. J. Mar. Biol. Assoc. 76, 749–757.